Adaptive and optimized COVID-19 vaccination strategies across geographical regions and age groups[*]

Jeta Molla[1], Alejandro Ponce de León Chávez[2], Takayuki Hiraoka[3], Tapio Ala-Nissila[4,5], Mikko Kivelä[3], and Lasse Leskelä[2]

[1]Department of Applied Physics, Aalto University, Otakaari 1, 02150 Espoo, Finland
[2]Department of Mathematics and Systems Analysis, Aalto University, Otakaari 1, 02150 Espoo, Finland
[3]Department of Computer Science, Aalto University, Konemiehentie 2, 02150 Espoo, Finland
[4]Quantum Technology Finland Center of Excellence and Department of Applied Physics, Aalto University, Otakaari 1, 02150 Espoo, Finland
[5]Interdisciplinary Centre for Mathematical Modelling and Department of Mathematical Sciences, Loughborough University, Loughborough, Leicestershire LE11 3TU, United Kingdom

May 27, 2021

Abstract

We evaluate the efficiency of various heuristic strategies for allocating vaccines against COVID-19 and compare them to strategies found using optimal control theory. Our approach is based on a mathematical model which tracks the spread of disease among different age groups and across different geographical regions, and we introduce a method to combine age-specific contact data to geographical movement data. As a case study, we model the epidemic in the population of mainland Finland utilizing mobility data from a major telecom operator. Our approach allows to determine which geographical regions and age groups should be targeted first in order to minimize the number of deaths. In the scenarios that we test, we find that distributing vaccines demographically and in an age-descending order is not optimal for minimizing deaths and the burden of disease. Instead, more lives could potentially be saved by using strategies which emphasize high-incidence regions and distribute vaccines in parallel to multiple age groups. The level of emphasis that high-incidence regions should be given depends on the overall transmission rate in the population. This observation highlights the importance of updating the vaccination strategy when the effective reproduction number changes due to the general contact patterns changing and new virus variants entering.

1 Introduction

With reports of around three million deaths and 160 million cases worldwide [2], the COVID-19 pandemic has caused a global public health crisis with far-reaching consequences to the economy and lives of people. Vaccines promise a way out of this situation, but due to limited supply and finite rate of vaccination they are not immediately effective in eradicating the epidemic. Health officials and governments around the world are thus faced with decisions on which order to vaccinate the population. This can be a matter of life and death to a large number of people and determine the speed at which we steer out of the crisis. The problem at hand is complicated by different mortality rates and activity levels in different age groups, localised incidence rates, and mobility patterns between regions, making it difficult to find an optimal solution on how to vaccinate using heuristic arguments. Given the scope of the crisis, even a small change in the relative efficiency of a strategy can have a large impact at the absolute scale in terms of saving lives. Therefore, critical evaluation on different vaccination strategies is imperative.

Several studies have previously explored the effectiveness of different age-structured vaccination strategies against the COVID-19 [7, 12, 13, 20, 21, 31]. Most of them agree that for minimizing cumulative incidence, i.e., the number of individuals who experience infection by the end of the epidemic, it is optimal to give priority to younger generations, as their higher activity accounts for a large part of the transmission. However, if the minimization of deaths and hospitalizations is targeted, it is often preferable to allocate vaccines first to the elderly who have a higher risk of severe illness and death. The set of strategies considered in the aforementioned studies is limited to sequential vaccinations of different age groups. They do not take into account parallel vaccination across age groups nor other factors such as the mobility and contact patterns of individuals. Further, suitable geographical distribution of vaccines is important especially when prevalence is inhomogeneously distributed across different geographical regions. Bertsimas et al. [4] and Grauer et al. [16] have shown that allocating vaccines to regions with high incidence can reduce the number of deaths compared to the strategy of distributing vaccines demographically. Ideally, all aforementioned factors should be optimized simultaneously, but once we start to take into account such parallel and region-based prioritization strategies, the space of possible strategies becomes so large that a brute-force search for an optimal strategy is no longer feasible; hence we need an efficient algorithm for finding a strategy that optimizes the given objective function.

To this end, we here construct an epidemic model that takes into account the various factors mentioned above. We use the model to study the effectiveness of different vaccination strategies by nonlinear optimization methods. The epidemic progression is described by a deterministic compartmental model adapted to COVID-19. As a case study, we adjust the model parameters to the recent epidemic situation on mainland Finland. Based on census data, age-structured contact patterns, and mobility patterns from a mobile phone operator, we infer contact patterns between individuals in different regions and age groups. Based on the available data of reported cases and vaccination counts, the performance of several vaccination strategies that are implemented or considered by health authorities is evaluated by means of a nonlinear programming framework. This framework allows us to optimize age-based and region-based vaccination schedules. As our main result, we find that the heuristic strategy of vaccinating the high-risk groups serially and distributing vaccines uniformly based on the local population density may not be optimal in minimizing deaths and mitigating the disease burden. Instead, better results can be obtained by parallel vaccination of different age groups and geographically targeted distribution of vaccines in a way that adapts to the ongoing incidence over time and takes into account demographic and behavioral differences

across different regions. This calls for re-evaluation of the details of any chosen vaccination strategy during the course of vaccinating the population.

2 Methods

The level of detail in modelling epidemic spreading dynamics depends both on the questions that need to be answered and the availability of relevant data. One of the characteristic features of the COVID-19 epidemic is the large heterogeneity in mortality across different age groups. For evaluating vaccination strategies, we also need to include the initial state of the epidemic at a given time, the arrival rate of new vaccine doses and their efficacy, and contact patterns between individuals of different ages for transmission rates. The final complication comes from geographic heterogeneity which requires local population densities and accurate mobility data between different regions. In this section we will give a concise summary of the model and the relevant data. Further details can be found in Appendix D.

Model

We introduce a deterministic compartmental model of COVID-19 transmission and vaccination which takes into account both heterogeneities across age groups and mobility across geographical regions. The model is an extended version of the one in Sjödin et al. [27] who modeled Sweden as a single region. In our model, mobility is incorporated so that each pair of regions has their own rates of commuting in the two directions, and commuting individuals may make infectious contacts both in their home region and in their target region. We assume that new vaccine doses arrive at a constant rate and all types of vaccines have equal efficacy. Vaccine efficacy is modelled using the all-or-nothing model in which some vaccinated individuals develop full immunity, and others none, 10 days after receiving the first dose [7, 27]. The proportion of individuals accepting to be vaccinated is assumed to be constant across the population. In our case study, the population is stratified into 9 age groups and 5 geographical regions (Table 1), giving us total of 45 age-region strata. Per each stratum, there are 13 epidemiological compartments, including three susceptible compartments (unvaccinated, vaccinated with developing immunity, and vaccinated without developing immunity) and two tracks (mild and severe) of infected individuals. This leads to a full model with 585 age-region-compartment combinations.

Data and initialization

The model is initialized to the epidemic situation in mainland Finland on the day of origin set to 18 April 2021. The age-structured population sizes were retrieved from national statistics [23]. The population sizes per region can be found at Table 1, and further details are in Appendix D. We build an age-dependent contact structure by adjusting a questionnaire-based contact matrix [22] to a setting where the age structure can vary between the geographical regions. Mobility between regions is estimated using aggregate tracking data from a major mobile phone operator.

The disease progression, vaccination, and hospitalization status in the age-region compartments is based mostly on data from Finnish health authorities [10]. With this data we initialize 8 out of 13 compartments for each age-region combination. The compartment related to deaths is set empty, so that the final results only consider new deaths after the initial date. Taking into account all age-region combinations, the model is initialized with 360 values.

Region	Population	Incidence	Vaccine uptake
HYKS	2 198 182	53.6	23.4
TYKS	869 004	39.9	26.9
TAYS	902 681	24.9	25.2
KYS	797 234	10.0	25.4
OYS	736 563	10.3	22.7
Total	5 503 664	34.7	24.4

Table 1: Population, incidence (7-day case notification rate per 100 000 individuals), and vaccine uptake (proportion of vaccinated with first dose per 100 individuals) in five regions (university hospital specific catchment areas) of mainland Finland on 18 April 2021.

Scenarios

The outcome of an epidemic depends on the future behavior of the population and other unknown factors which are difficult if not impossible to properly include in modeling. To account for such factors we run several different scenarios. The amount of social activity and the tendency for the disease to spread can both be absorbed to the overall rate of infectious contacts. We calibrate this in a way that the effective reproduction number in the model gets a range of values $R_{\text{eff}} \in \{0.75, 1.0, 1.25, 1.50\}$ (see Appendix A.4). Here $R_{\text{eff}} = 1.0$ corresponds to the case where without any further vaccinations, the number of infected people would remain roughly constant at short time scales before natural immunity is increased by newly recovered individuals. Lower values indicate that the disease will naturally shrink, and higher values mean that the incidence would increase in the absence of any further vaccinations. In all scenarios, the arrival rate of new vaccine doses is set to 30 000 per day.

The amount of cross-region mobility and the fraction of contacts that are made at commuting destinations is difficult to estimate reliably and is prone to change in the future. As a sensitivity test, we investigate the impact of cross-region mobility by running numerical experiments in three different simplified scenarios: no mobility ($\tau = 0$), medium-level mobility ($\tau = 0.5$), and high-level mobility ($\tau = 1$).

Heuristic vaccination strategies

We construct heuristic vaccination strategies which can depend on three variables for each region k and given time t: the proportion of population $\hat{N}_k$, the proportion of new infections $\hat{I}_k^D(t)$ during the last D days, and the proportion of hospitalized individuals $\hat{H}_k^D(t)$ during the last D days in region k. Given that there are in total $v(t)$ vaccine doses to distribute on day t, the region k will receive

$$v_k(t) = v(t)\Big(w_1 \hat{N}_k + w_2 \hat{I}_k^D(t) + w_3 \hat{H}_k^D(t)\Big) \tag{2.1}$$

vaccine doses. The choice of weights w_1, w_2, and w_3 determines the relative allocation of vaccines across regions, with $w_1 + w_2 + w_3 = 1$. Within regions, the $v_k(t)$ vaccine doses are distributed in an age-prioritized strategy from older to younger age groups. We set $D = 14$ and build 8 different vaccination strategies by setting the w_i values as shown in Table 2. See Appendix B for further details. The feasibility of implementing strategy Pop+Inc+Hosp corresponding to equal weights $w_1 = w_2 = w_3$ has been discussed by Finnish health authorities [11].

4

Strategy	w_1	w_2	w_3
Pop	1	0	0
Inc	0	1	0
Hosp	0	0	1
Pop+Hosp	1/2	0	1/2
Pop+Inc	1/2	1/2	0
Inc+Hosp	0	1/2	1/2
Pop+Inc+Hosp	1/3	1/3	1/3

Table 2: Adaptive vaccination strategies and their corresponding weights corresponding to (2.1). Pop, Inc and Hosp refer to strategies where vaccines are distributed demographically, based on the regional incidence level only, and based on the number of hospitalized cases only, respectively.

Optimized vaccination strategies

In order to obtain an optimized age-specific and time-dependent vaccination strategy, we formulate the problem in terms of optimal control theory with the aim of minimizing the total number of deaths while satisfying the constraints of a fixed daily maximum amount of vaccines available over the course of a single pandemic wave. To numerically solve the optimal control problem, we convert it into a finite-dimensional nonlinear optimization problem (NLP) [5, 26]. The numerical implementation of the NLP is done using a sequential least squares programming (SLSQP) algorithm [30]. In addition to the objective function value, the SLSQLP algorithm requires the gradients of the NLP with respect to the minimization variable which we calculate based on Pontryagin's Maximum Principle [17, 18]. This approach gives us a local optimization method which means that the algorithm may converge to different optimal strategies depending on the initialization. We consider the no-vaccination strategy and several heuristic strategies for initializing the algorithm and choose the vaccination strategy for which the algorithm reaches a minimum of the objective function. The details are given in Appendix C.

3 Results

We summarise our results by focusing on the medium-level mobility scenario. The relative performance of different vaccination strategies and their qualitative behavior is robust across different mobility levels (see Appendix E). Furthermore, reduced cross-region mobility significantly reduces the overall spread and severity of the epidemic.

The code used for doing the analysis and producing the results in this paper is publicly available as a Github repository[1].

Comparison of adaptive heuristic strategies

We first compare different vaccination strategies at the level of the whole country to a baseline strategy Pop (Fig. 1) in which vaccine doses are first allocated to regions weighted by population counts, and then serially to age groups in descending order within each region. This static baseline strategy differs from all other strategies which we call *adaptive heuristic strategies* in a way that it

---

[1]https://github.com/FINCoVID19/optimized_vaccination_finland

does not try to adapt to the evolution of the epidemic in any way. The adaptive heuristic strategies allocate more vaccine doses to regions with more infections and/or hospitalizations, but are similarly age-prioritized within regions.
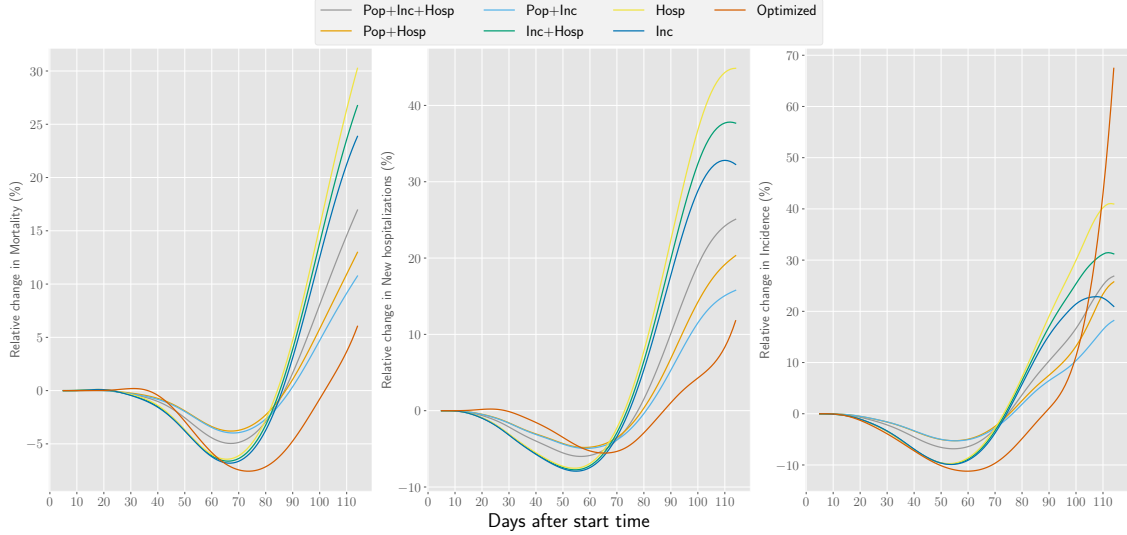

Figure 1: Relative change in mortality, hospitalizations, and incidence for the vaccination strategies in Table 2 with respect to the baseline strategy `Pop`. In this scenario, the effective reproduction number is $R_{\text{eff}} = 1.5$ and the mobility value is $\tau = 0.5$. For other parameter combinations, see Appendix E.

Figure 1 describes the relative performance of different strategies over time, assessed by reduction in the daily number of deaths, hospitalizations, and incidence. Overall, the adaptive heuristic strategies outperform the baseline in short time scales but do worse in long time scales. This is because the adaptive heuristics delay the epidemic and its peak as compared to the baseline, and eventually the less-vaccinated regions in the adaptive heuristics will do worse than in the baseline strategy. This can be further seen in Fig. 2 which shows the evolution of mortality in each region.

Whether or not it pays off to delay the epidemic with adaptive strategies at the cost of allocating less vaccines to less affected regions depends on how fast the disease is progressing. Specifically, the total performance over the full time horizon depends on the transmission rates of the disease (see Table 3): In low-transmission scenarios the adaptive heuristics perform well and delaying the epidemic can be beneficial because there is time to develop additional immunity in the low-incidence regions to hinder future spreading. In high-transmission scenarios the adaptive heuristics put too much emphasis on the initially high-incidence regions and leave the low-incidence regions vulnerable to large future outbreaks.

As expected, none of the strategies can outperform the baseline in every region. The regions that have initially less incidence will suffer on the expense of the high-incidence regions when changing from the baseline strategy to adaptive strategies. However, as stated before, if all individuals in the country are treated equally regardless of their region of residence, the transmission rate will determine which strategy is best for minimizing the total disease-induced mortality in the country.
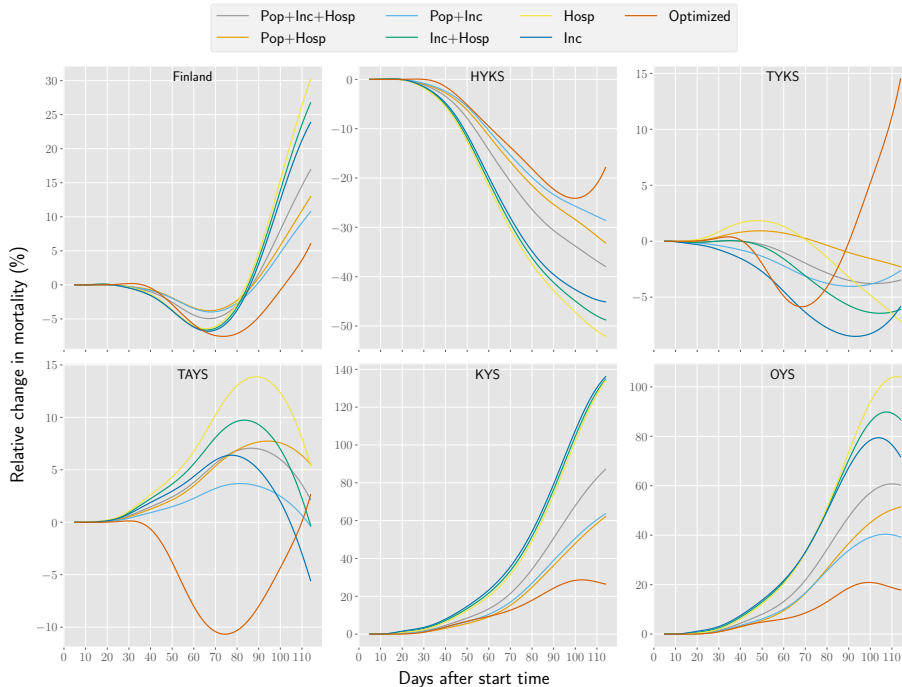
Figure 2: Relative change in mortality in Finland and the five hospital catchment areas included here for the vaccination strategies in Table 2 with respect to vaccination strategy `Pop`. For this scenario, the basic reproduction number $R_{\text{eff}} = 1.5$ and the mobility value $\tau = 0.5$. For other parameter values combinations, see Appendix E.

Among the adaptive vaccination strategies, the number of hospitalized individuals is not in general as good a measure as incidence when determining where to distribute the vaccines. This might be due to the delay in the hospitalization which means that vaccination continues in regions where the effective reproduction number is already low, at the expense of regions where incidence is on the rise but not yet reflected in hospitalizations.

It should be noted that in our model the number of daily new infections is assumed to be accurately reported, which is not a realistic assumption. While it does not make any difference for the strategy if the total numbers are systematically lower due to underreporting, fluctuations in the numbers and systematic biases in the measurements across regions could have an impact.

Performance of optimized vaccination strategies

We will next discuss the performance of an optimized vaccination strategy found by running the numerical algorithm described in Section 2 with the objective of minimizing the total disease-induced mortality over a 115-day time horizon. Our numerical results indicate that the optimized strategy shares good features of both the static baseline strategy and the adaptive heuristic strategies: There is an initial drop in mortality similar to heuristic strategies, but in the long term the difference to baseline is not as large as for the heuristic strategies. In other words, at later times of the epidemic
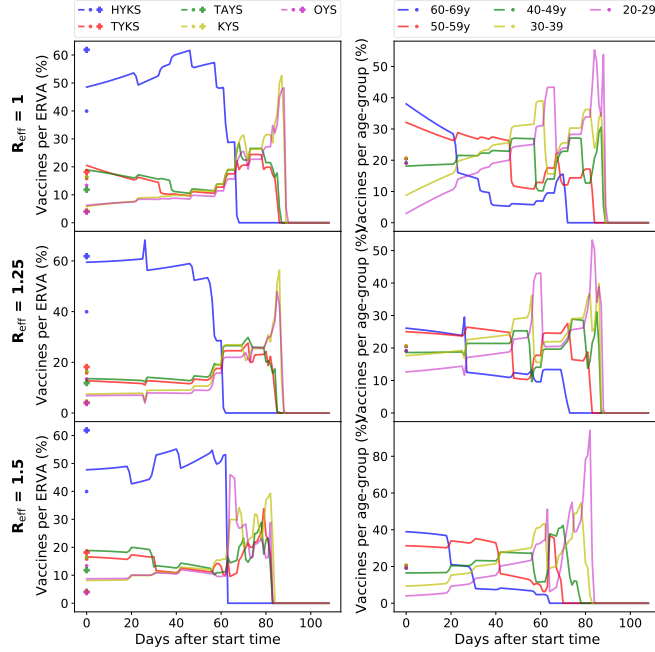
Figure 3: Percentage of vaccine doses allocated by the optimized strategy to regions (left) and age groups (right) in three scenarios ($R_{\text{eff}} = 1, 1.25, 1.5$). On the left, dots and crosses represent the percentage of vaccines which each region would receive with `Pop` (baseline) and `Inc` strategies, respectively. On the right, dots stand for the percentage which each age group would receive if vaccines were distributed proportionally to age group sizes.

the optimized strategy demonstrates the highest reduction in mortality. Overall, the optimized strategy shows reduction in mortality by up to 70 individuals for $R_{\text{eff}} = 1.5$ (see Table 3). The reason why the differences in mortality are not very large is because the majority of individuals in high-risk groups have already been vaccinated in the beginning of the calculations (18 April 2021). However, cumulative incidence can reach differences of up to tens of thousands, as Table 3 shows.

The percentage of vaccine doses allocated by the optimized strategy to each geographical region and age group is shown in Fig. 3 for three transmission scenarios. Similarly to the heuristic strategies, the optimized strategy depends heavily on the disease parameters. The effective reproduction number does not just fine-tune the strategy, but there is a transition from one approach to another: For a low-transmission scenario ($R_{\text{eff}} = 0.75$) in which the epidemic is in clear decline, the optimized strategy does not preferentially target older age groups but tries to reduce the number of infections, and the optimized strategy is the one that follows the number of infected. In scenarios with a high overall transmission rate, the optimized strategy favours older age groups having higher risk of severe illness and death.

Both the low-transmission and high-transmission scenarios lead to an optimized strategy that

8

favours the initially high-incidence region, and this effect is stronger for low-transmission scenarios. Specifically, the optimized strategy initially targets the capital region (HYKS) with approximately 20 (resp. 8) percentage points higher share of available vaccine doses than the baseline strategy for $R_{\text{eff}} = 1.25$ (resp. 1.5). Interestingly, the optimization finds that the age prioritization is smaller and geography prioritization more aggressive in the scenario with $R_{\text{eff}} = 1.25$ than in scenarios with $R_{\text{eff}} = 1.0$ and $R_{\text{eff}} = 1.5$.

	R_{eff}	Hosp	Inc	Inc+Hosp	Pop+Hosp	Pop+Inc	Pop+Inc+Hosp	Optimized
Mortality	0.75	-0.38	**-0.42**	-0.40	-0.23	-0.25	-0.31	**-0.42**
	1.00	-3.07	-3.45	-3.27	-2.02	-2.17	-2.57	**-3.69**
	1.25	-9.63	-14.16	-12.04	-9.86	-11.52	-11.82	**-27.10**
	1.50	58.44	30.51	43.63	10.21	-0.47	15.88	**-70.48**
Incidence	0.75	-351.17	-352.77	-351.58	-181.80	-181.61	-239.02	**-580.45**
	1.00	-2308.30	-2448.11	-2381.21	-1387.21	-1415.68	-1753.48	**-3159.17**
	1.25	-5884.04	-8884.67	-7464.80	-5686.31	-6505.21	-6752.67	**-20750.36**
	1.50	15340.54	1183.97	7928.77	2964.71	-1931.73	3304.50	**-30546.26**

Table 3: Absolute difference in mortality and incidence resulting from different vaccination strategies with respect to baseline strategy (Pop) for $\tau = 0.5$. Highest reductions are indicated in boldface. Results for different values of τ are shown in Appendix E, Table 15 including hospitalizations.

4 Discussion and conclusions

In this work we have constructed an epidemic modelling framework which allows to evaluate various adaptive strategies for allocating vaccines based on static demographic data and dynamic evolution of the epidemic situation across different geographical regions. We investigated various heuristic strategies for allocating more vaccines to regions with higher incidence and hospital load, together with optimized strategies which may flexibly allocate vaccines to different age groups and regions in parallel. Our numerical results, conducted for scenarios adjusted to the recent COVID-19 epidemic situation in Finland, show that optimized vaccination strategies can reduce the death toll and significantly mitigate the disease burden of the epidemic. The relative advantage of different adaptive strategies over the static baseline is influenced by the overall epidemic situation. Also, whatever strategy is chosen, a trade-off between different regions is inevitable due to limited supply of vaccine doses and daily vaccination capacity. Nevertheless, the results provide valuable insights for designing efficient vaccination strategies: In general, using hospital loads as basis in allocating vaccine doses tends to lead to worse performance compared to the static baseline. The optimized strategy appears to achieve a good balance between short-term benefits of adaptive strategies and the long-term robustness gained by the uniform vaccine allocation. Further, even though we optimize mortality, there is a delicate balance between favoring individuals with higher direct risk of death as opposite to individuals at risk of getting infected and causing large outbreaks.

As with all modelling, there are several factors and phenomena that are not included, and the results can change if these factors turn out to be important. Typically this would imply that the actual numbers in a modelling study might be subject to change, but the overall phenomena that are observed here are relatively robust. Such numbers would be the exact number of infected, hos-

pitalized, and deceased individuals, and the phenomena the relative order of the different strategies. The only real way of knowing which factors are important is to include them in a model, but in practice the choice of relevant factors is informed by the reliability of the model. This is why we have chosen to start with a model benchmarked in another study related to Sweden [27], and modify it by making it more accurate by including geographical information.

There are several factors which we believe that are missing in our model and are important for both the accuracy of the results and important to consider when optimizing vaccination strategies. First is the need for more than a single vaccine dose needed by many of the currently used vaccines, which is not modelled here. Including this in the model would allow one to optimize the vaccination strategy further by finding an optimal strategy for giving the second dose with relation to vaccinating different age groups and geographical locations. Second, one should allow the infectious contact rates to change across geographical regions and time. As the public is informed of the current pandemic situation their behavior, and therefore the transmission rate, is bound to change. This induces a feedback loop which makes a large difference especially for long-term predictions, but also makes modeling more difficult as one needs to model the public response to various pandemic situations [14, 15]. In addition, the governments will take actions given that the situation is sufficiently critical [24], and these decisions might depend on several hard-to-model factors related to politics.

Studying the effects of cross-region mobility were not at the main focus of this study, but the sensitivity analysis that we performed for the overall mobility factor has interesting implications. It turned out that cross-region mobility can be an important factor even in this relatively advanced state of the epidemic where all regions have some incidence, but there is still a geographical imbalance in the relative incidences. These results are especially striking considering that the mobility factor τ only controls for cross-region mobility but not the overall contact rates of the individuals. That is, decreasing τ decreases the cross-region contacts but increases the inside-region contacts, and the total rate of contacts in the country remains the same but the large-scale geographical mixing patterns changed. This is in contrast to conventional models which assume full mixing across the country. Further, these findings could have implications on interventions that limit long-range mobility. Further research in this direction would be needed for concluding about these type of interventions.

Our analysis reveals that designing efficient vaccination strategies at a level of a country is highly nontrivial. As seen from our results in Fig. 3, the details of optimized strategies can be complicated and their faithful implementation difficult. However, it should be possible to simplify the strategies and try to follow the main principles of parallel vaccination and geographic distribution of vaccines with as much detail as practically possible. It is important to note that carefully analyzed and executed strategies can potentially save lives even if the strategy is changed after most of the risk groups are already vaccinated. Much larger effects could potentially be obtained if the planning were done before vaccinations started, but in this case the problem is that the various parameters related to vaccination efficiency might not be known. In any case, the relative performance of different strategies can depend on the effective reproduction number, which means that the vaccination strategy should be chosen in conjunction with non-pharmaceutical intervention strategies of the country.

References

[1] Helsingin Sanomat, Hospitalized data API, April 2021. API: https://w3qa5ydb4l.execute-api.eu-west-1.amazonaws.com/prod/finnishCoronaHospitalData. Repository:

`https://github.com/HS-Datadesk/koronavirus-avoindata`.

[2] The Johns Hopkins Coronavirus Resource Center, April 2021. `https://coronavirus.jhu.edu`.

[3] S. Arregui, A. Aleta, J. Sanz, and Y. Moreno. Projecting social contact matrices to different demographic structures. *PLOS Computational Biology*, 14(12):1–18, 12 2018.

[4] D. Bertsimas, J. K. Ivanhoe, A. Jacquillat, M. L. Li, A. Previero, O. S. Lami, and H. T. Bouardi. Optimizing Vaccine Allocation to Combat the COVID-19 Pandemic. *medRxiv*, 2020.

[5] J. T. Betts. *Practical Methods for Optimal Control and Estimation Using Nonlinear Programming*. Society for Industrial and Applied Mathematics, 2010.

[6] F. Brauer, C. Castillo-Chavez, and Z. Feng. *Mathematical Models in Epidemiology*. Springer, 2019.

[7] K. M. Bubar, K. Reinholt, S. M. Kissler, M. Lipsitch, S. Cobey, Y. H. Grad, and D. B. Larremore. Model-informed COVID-19 vaccine prioritization strategies by age and serostatus. *Science*, 371(6532):916–921, 2021.

[8] O. Diekmann, H. Heesterbeek, and T. Britton. *Mathematical Tools for Understanding Infectious Disease Dynamics*. Princeton University Press, 2012.

[9] O. Diekmann, J. A. P. Heesterbeek, and M. G. Roberts. The construction of next-generation matrices for compartmental epidemic models. *Journal of the Royal Society Interface*, 7(47), 2010.

[10] Finnish Institute for Health and Welfare (THL). COVID-19 API, April 2021. API: `https://sampo.thl.fi/pivot/prod/en/epirapo/covid19case/fact_epirapo_covid19case`. Instructions: `https://thl.fi/en/web/thlfi-en/statistics/statistical-databases/open-data/confirmed-corona-cases-in-finland-covid-19-`.

[11] Finnish Institute of Health and Welfare (THL). Regional allocation of covid-19 vaccines (in Finnish), March 2021. `https://thl.fi/documents/10531/6950916/Covid+-19+rokoteannosten+alueellinen+kohdennus_THL+lausunto_20210325_val....pdf/85fc9e04-0796-d222-2911-b99867a07158?t=1616760195281`.

[12] B. Goldenbogen, S. O. Adler, O. Bodeit, J. A. Wodke, X. Escalera-Fanjul, A. Korman, M. Krantz, L. Bonn, R. Morán-Torres, J. E. Haffner, M. Karnetzki, I. Maintz, L. Mallis, H. Prawitz, P. S. Segelitz, M. Seeger, R. Linding, and E. Klipp. Optimality in COVID-19 vaccination strategies determined by heterogeneity in human-human interaction networks. *medRxiv*, 2020.

[13] J. R. Goldstein, T. Cassidy, and K. W. Wachter. Vaccinating the oldest against COVID-19 saves both the most lives and most years of life. *Proceedings of the National Academy of Sciences*, 118(11):e2026322118, 2021.

[14] N. Gozzi, D. Perrotta, D. Paolotti, and N. Perra. Towards a data-driven characterization of behavioral changes induced by the seasonal flu. *PLoS Computational Biology*, 16(5):e1007879, 2020.

11

[15] N. Gozzi, M. Scudeler, D. Paolotti, A. Baronchelli, and N. Perra. Self-initiated behavioural change and disease resurgence on activity-driven networks. *arXiv*, 2020.

[16] J. Grauer, H. Löwen, and B. Liebchen. Strategic spatiotemporal vaccine distribution increases the survival rate in an infectious disease like COVID-19. *Scientific Reports*, 10(1):1–10, 2020.

[17] S. Li, R. Zhao, and Q. Zhang. Optimization method for solving bang-bang and singular control problems. *Journal of Control Theory and Applications*, 10(4):559–564, 2012.

[18] J. Macki and A. Strauss. *Introduction to Optimal Control Theory*. Springer, 2012.

[19] S. A. Madhi, V. Baillie, C. L. Cutland, M. Voysey, A. L. Koen, L. Fairlie, S. D. Padayachee, K. Dheda, S. L. Barnabas, Q. E. Bhorat, et al. Efficacy of the ChAdOx1 nCoV-19 Covid-19 vaccine against the B. 1.351 variant. *New England Journal of Medicine*, 2021.

[20] L. Matrajt, J. Eaton, T. Leung, and E. R. Brown. Vaccine optimization for COVID-19: Who to vaccinate first? *Science Advances*, 7(6):eabf1374, 2020.

[21] S. Moore, E. M. Hill, L. Dyson, M. J. Tildesley, and M. J. Keeling. Modelling Optimal Vaccination Strategy For SARS-CoV-2 in the UK. *medRxiv*, 2020.

[22] J. Mossong, N. Hens, M. Jit, P. Beutels, K. Auranen, R. Mikolajczyk, M. Massari, S. Salmaso, G. S. Tomba, J. Wallinga, J. Heijne, M. Sadkowska-Todys, M. Rosinska, and W. J. Edmunds. Social Contacts and Mixing Patterns Relevant to the Spread of Infectious Diseases. *PLOS Medicine*, 5(3), 03 2008.

[23] Official Statistics of Finland. Population structure database, April 2021. API: https://pxnet2.stat.fi/PXWeb/pxweb/en/StatFin/StatFin__vrm__vaerak/statfin_vaerak_pxt_11re.px/.

[24] N. Perra. Non-pharmaceutical interventions during the COVID-19 pandemic: A review. *Physics Reports*, 2021.

[25] F. P. Polack, S. J. Thomas, N. Kitchin, J. Absalon, A. Gurtman, S. Lockhart, J. L. Perez, G. Pérez Marc, E. D. Moreira, C. Zerbini, R. Bailey, K. A. Swanson, S. Roychoudhury, K. Koury, P. Li, W. V. Kalina, D. Cooper, R. W. Frenck, L. L. Hammitt, Ö. Türeci, H. Nell, A. Schaefer, S. Ünal, D. B. Tresnan, S. Mather, P. R. Dormitzer, U. Şahin, K. U. Jansen, and W. C. Gruber. Safety and efficacy of the BNT162b2 mRNA covid-19 vaccine. *New England Journal of Medicine*, 383(27):2603–2615, 2020. PMID: 33301246.

[26] A. Rao. A survey of numerical methods for optimal control. *Advances in the Astronautical Sciences*, 135(1):497–528, 2009.

[27] H. Sjödin, J. Rocklöv, and T. Britton. Evaluating and optimizing COVID-19 vaccination policies: A case study of Sweden. *medRxiv*, 2021.

[28] M. G. Thompson, J. L. Burgess, A. L. Naleway, H. L. Tyner, S. K. Yoon, J. Meece, L. E. Olsho, A. J. Caban-Martinez, A. Fowlkes, K. Lutrick, et al. Interim estimates of vaccine effectiveness of BNT162b2 and mRNA-1273 COVID-19 vaccines in preventing SARS-CoV-2 infection among health care personnel, first responders, and other essential and frontline workers-eight US locations, December 2020–March 2021. *Morbidity and Mortality Weekly Report*, 70(13):495, 2021.

[29] E. Vasileiou, C. R. Simpson, C. Robertson, T. Shi, S. Kerr, U. Agrawal, A. Akbari, S. Bedston, J. Beggs, D. Bradley, et al. Effectiveness of first dose of COVID-19 vaccines against hospital admissions in Scotland: National prospective cohort study of 5.4 million people. *SSRN*, 2021.

[30] P. Virtanen, R. Gommers, T. E. Oliphant, M. Haberland, T. Reddy, D. Cournapeau, E. Burovski, P. Peterson, W. Weckesser, J. Bright, S. J. van der Walt, M. Brett, J. Wilson, K. J. Millman, N. Mayorov, A. R. J. Nelson, E. Jones, R. Kern, E. Larson, C. J. Carey, İ. Polat, Y. Feng, E. W. Moore, J. VanderPlas, D. Laxalde, J. Perktold, R. Cimrman, I. Henriksen, E. A. Quintero, C. R. Harris, A. M. Archibald, A. H. Ribeiro, F. Pedregosa, P. van Mulbregt, and SciPy 1.0 Contributors. SciPy 1.0: Fundamental Algorithms for Scientific Computing in Python. *Nature Methods*, 17:261–272, 2020.

[31] W. Wang, Q. Wu, J. Yang, K. Dong, X. Chen, X. Bai, X. Chen, Z. Chen, C. Viboud, M. Ajelli, and H. Yu. Global, regional, and national estimates of target population sizes for COVID-19 vaccination: Descriptive study. *BMJ*, 371:m4704, dec 2020.

A Model description

A.1 Population strata

The population of a country is modelled as a closed system of N individuals, divided into regions $k = 1, \ldots, K$ and age groups $g = 1, \ldots, G$. An individual resident in region k in age group g is called a kg-individual, and the number of such individuals is denoted by N_{kg}. In what follows, g, h always refer to age, and k, ℓ, m to regions. The population size of region k is denoted by $N_k = \sum_g N_{kg}$, and the size of age group g by $N_g = \sum_k N_{kg}$. These numbers are listed in Table 6.

Vaccine protection is modelled using the all-or-nothing model in which a certain fraction of vaccinated receive full immunity, and the rest no immunity. The population in each stratum is divided into 13 time-dependent epidemiological compartments described in Table 4. In the special case with only one region, this model reduces to the one studied in [27].

A.2 Spatial evolution equations

Symbol	Description
S^u	Susceptible, unvaccinated
S^v	Susceptible, invited for vaccination
S^x	Susceptible, vaccinated with no immunity or declined vaccination
E	Infected but not yet infectious
I	Infected and infectious
Q^0	Quarantined at home, mild disease
Q^1	Quarantined at home, severe disease
H^w	hospitalized, in general ward
H^c	hospitalized, in critical care
H^r	hospitalized, in recovery ward
D	Deceased
R	Recovered with full immunity
V	Vaccinated with full immunity

Table 4: Epidemiological compartments. There are KG copies of each compartment, denoted $S^u_{kg}, S^v_{kg}, \ldots, V_{kg}$ for regions $k = 1, \ldots, K$ and age groups $g = 1, \ldots, G$.

The dynamics of the disease is modelled using a deterministic nonlinear system of $13KG$ ordinary differential equations with structure shown in Fig. 4. Each node in the diagram corresponds to one differential equation with the time derivative of the associated variable on the left side, the values of the source nodes of incident arrows on the right side, each incoming arrow equipped with a plus sign, and each outgoing arrow equipped with a minus sign. We treat these numbers as expected values, so they may take noninteger values. This leads to a system where susceptible compartments evolve according to

$$\begin{aligned}
\frac{d}{dt} S^u_{kg} &= -\lambda_{kg} S^u_{kg} - v_{kg} S^u_{kg}, \\
\frac{d}{dt} S^v_{kg} &= v_{kg} S^u_{kg} - \lambda_{kg} S^v_{kg} - \frac{1}{T_V} S^v_{kg}, \\
\frac{d}{dt} S^x_{kg} &= (1 - \alpha e) \frac{1}{T_V} S^v_{kg} - \lambda_{kg} S^x_{kg},
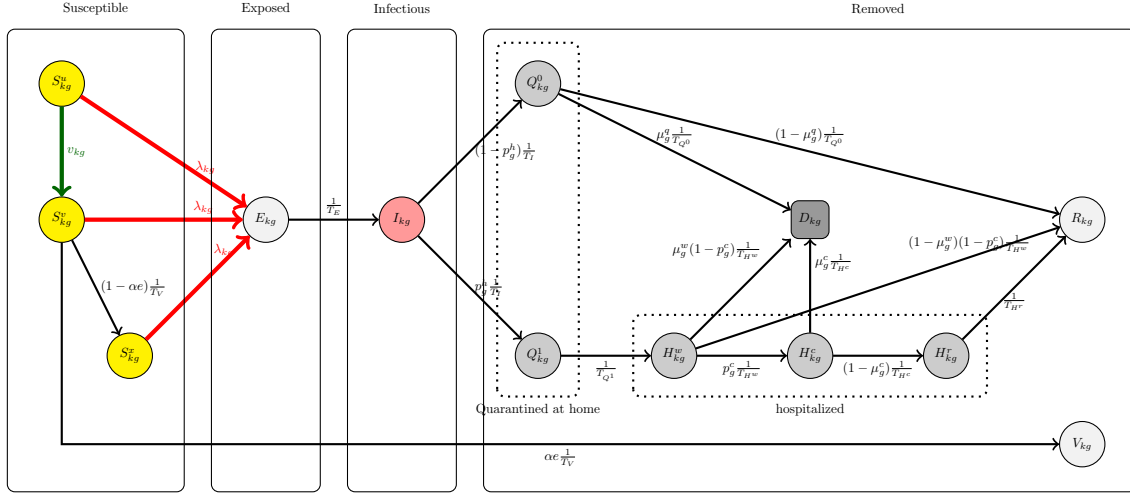\end{aligned} \tag{A.1}$$

Figure 4: Disease transmission dynamics.

infected but noninfectious compartments according to

$$\frac{d}{dt}E_{kg} = \lambda_{kg}(S_{kg}^u + S_{kg}^v + S_{kg}^x) - \frac{1}{T_E}E_{kg}, \tag{A.2}$$

infectious compartments according to

$$\frac{d}{dt}I_{kg} = \frac{1}{T_E}E_{kg} - \frac{1}{T_I}I_{kg}, \tag{A.3}$$

and removed compartments according to

$$
\begin{aligned}
\frac{d}{dt}Q_{kg}^0 &= (1 - p_g^h)\frac{1}{T_I}I_{kg} - \frac{1}{T_{Q^0}}Q_{kg}^0, \\
\frac{d}{dt}Q_{kg}^1 &= p_g^h\frac{1}{T_I}I_{kg} - \frac{1}{T_{Q^1}}Q_{kg}^1, \\
\frac{d}{dt}H_{kg}^w &= \frac{1}{T_{Q^1}}Q_{kg}^1 - \frac{1}{T_{H^w}}H_{kg}^w, \\
\frac{d}{dt}H_{kg}^c &= p_g^c\frac{1}{T_{H^w}}H_{kg}^w - \frac{1}{T_{H^c}}H_{kg}^c, \\
\frac{d}{dt}H_{kg}^r &= (1 - \mu_g^c)\frac{1}{T_{H^c}}H_{kg}^c - \frac{1}{T_{H^r}}H_{kg}^r, \\
\frac{d}{dt}R_{kg} &= (1 - \mu_g^q)\frac{1}{T_{Q^0}}Q_{kg}^0 + (1 - \mu_g^w)(1 - p_g^c)\frac{1}{T_{H^w}}H_{kg}^w + \frac{1}{T_{H^r}}H_{kg}^r, \\
\frac{d}{dt}D_{kg} &= \mu_g^q\frac{1}{T_{Q^0}}Q_{kg}^0 + \mu_g^w(1 - p_g^c)\frac{1}{T_{H^w}}H_{kg}^w + \mu_g^c\frac{1}{T_{H^c}}H_{kg}^c, \\
\frac{d}{dt}V_{kg} &= \alpha e\frac{1}{T_V}S_{kg}^v.
\end{aligned}
\tag{A.4}
$$

In formulae (A.1)–(A.4), the force of infection inflicted on kg susceptibles $\lambda_{kg} = \lambda_{kg}(t)$ varies over time as a function of infectious states in all strata and additional parameters. The force of infection

(per capita rate of infections) inflicted on susceptible kg individuals equals

$$\lambda_{kg}(I) \;=\; \beta \sum_{m,\ell,h} \frac{\beta_{gh}}{\hat{N}_m} \theta_{km} I_{\ell h} \theta_{\ell m}, \tag{A.5}$$

where β is a constant used for adjusting the overall rate of infectious contacts, (β_{gh}) is a 9-by-9 mobility-adjusted age contact matrix described in Section A.5, $(\theta_{k\ell})$ is a 5-by-5 baseline mobility matrix described in Section A.3, and $\hat{N}_m$ is the effective population size of region m, see Section A.3. This corresponds to a model where $\beta \times \beta_{gh}/\hat{N}_m$ is the contact rate between any unordered pair of individuals present in region m, with one individual belonging to age group g and the other to age group h.

The per-capita rate of vaccines offered to residents of region k in age group g is a time-dependent function $v_{kg} = v_{kg}(t)$ obtained as a solution of a minimization problem described in Section C, or defined manually corresponding to vaccination strategies listed in Table 2. The other model parameters are constant and are listed in Table 5.

A.3   Mobility

Mobility of individuals is modelled using a Lagrangian approach [6] using a K-by-K probability matrix where entry $\theta_{k\ell}$ equals the fraction of time that a typical resident of region k spends in region ℓ. Then

$$\hat{N}_{\ell g} \;=\; \sum_{k} N_{kg} \theta_{k\ell} \tag{A.6}$$

equals the mean number of individuals of age group g present in region ℓ, and

$$\hat{N}_{\ell} \;=\; \sum_{g} \hat{N}_{\ell g}$$

represents the mean number of individuals present in region ℓ.

The baseline mobility matrix representing typical mobility in Finland during normal times without pandemic is a 5-by-5 matrix with entries estimated from available data on cross-region travels as

$$\theta_{k\ell} \;=\; \left((1-\tau) + \tau\left(1 - \frac{T_{k+}}{N_k}\right)\right)\delta_{k\ell} + \tau\frac{T_{k+}}{N_k}\frac{T_{k\ell}}{T_{k+}}(1-\delta_{k\ell}), \tag{A.7}$$

where $T_{k+} = \sum_{\ell \neq k} T_{k\ell}$, $(T_{k\ell})$ is an estimated trip matrix with $T_{k\ell}$ telling the daily number of trips that residents of region k make to region ℓ in Table 8, and N_k is the number of residents in region k obtained from Table 6. The parameter τ represents the fraction daily activity time that a typical commuter spends in a remote region. In our numerical simulations we set $\tau = \{0, 0.5, 1\}$ due to lack of reliable data for estimating this factor. Equation (A.7) can be interpreted as the expected fraction of active day time that a resident of region k spends in region ℓ, with T_{k+}/N_k being the probability that a randomly selected resident of region k commutes outside the home region on a given day.

A.4   Calibration of the overall infectious contact rate

The overall infectious contact rate parameter β is parameterised in terms of an effective reproduction number R_{eff} as follows. Denote by $K^{(\beta)}$ a KG-by-KG matrix with entries

$$K^{(\beta)}_{kg,\ell h} \;=\; \beta T_I S_{kg}(0) M_{kg,\ell h},$$

16

where

$$M_{kg,\ell h} \;=\; \beta_{gh} \sum_m \frac{\theta_{km}\theta_{\ell m}}{\hat{N}_m},$$

and $S_{kg}(0) = S_{kg}^u(0) + S_{kg}^v(0) + S_{kg}^x(0)$ is the number of kg susceptibles at time zero. Then $K_{kg,\ell h}^{(\beta)}$ indicates the expected number of new infections among kg individuals caused by an infectious ℓh individual during its infectious lifetime, which got infected at time zero. Then we set

$$\beta \;=\; \frac{R_{\text{eff}}}{\rho(K^{(1)})},$$

where $\rho(K^{(1)})$ is the spectral radius of the matrix $K^{(1)} = T_I S_{kg}(0) M_{kg,\ell h}$, and R_{eff} is set to values 0.75, 1.0, 1.25, 1.50 in different scenarios. With this choice, the spectral radius of $K^{(\beta)}$ equals $\rho(K^{(\beta)}) = R_{\text{eff}}$, and $R_{\text{eff}} < 1$ (resp. $R_{\text{eff}} > 1$) indicates the convergence to zero (resp. divergence) of a subsystem of differential equations

$$\frac{d}{dt}E_{kg} \;=\; \beta S_{kg}(0) \sum_{\ell h} M_{kg,\ell h} I_{\ell h} - \frac{1}{T_E} E_{kg},$$

$$\frac{d}{dt}I_{kg} \;=\; \frac{1}{T_E} E_{kg} - \frac{1}{T_I} I_{kg},$$

only containing the infectious compartments, linearised in a neighbourhood of a stable initial state where $S_{kg}^u(0), S_{kg}^v(0), S_{kg}^x(0)$ are fixed to their current states, and $E_{kg} = I_{kg} = 0$ for all kg, see [8, 9]. Hence $R_{\text{eff}} < 1$ indicates that all infectious compartments would decrease locally in time even without future vaccinations. In the special case where $S_{kg}(0) = N_{kg}$ for all kg, R_{eff} reduces to the basic reproduction number. In general this not the case because R_{eff} also takes into account the accumulated immunity at time zero due to prior vaccinations and recovery.

A.5 Pair contact rates

Contacts between individuals are modelled so that $\beta_{gh}/\hat{N}_m$ denotes the mean contact rate (unnormalized, corresponding to no pandemic) in region m between any unordered pair of individuals present in region m, such that one individuals is in age group g and the other in age group h. The expected number of such pairs equals

$$\hat{E}_{gh}^{(m)} \;=\; \begin{cases} \hat{N}_{mg}\hat{N}_{mh}, & g \neq h; \\ \frac{1}{2}\hat{N}_{mg}^2 - \frac{1}{2}\sum_k N_{kg}\theta_{km}^2, & g = h, \end{cases} \tag{A.8}$$

when we assume that each resident of each region k is present in region m with probability θ_{km}, independently of the other individuals (see Section A.5.1 below for details). Then the aggregate rate of contacts between age groups g and h is given by $\beta_{gh}E_{gh}$, where

$$E_{gh} \;=\; \sum_m \frac{\hat{E}_{gh}^{(m)}}{\hat{N}_m}$$

is a mobility correction factor. The aggregate contact rate between age groups g and h can alternatively be computed as $(1 - \frac{1}{2}\delta_{gh})N_g C_{gh}$, where N_g is the size of age group g and C_{gh} is the age

17

contact matrix. By solving the balance equation $(1 - \frac{1}{2}\delta_{gh})N_g C_{gh} = \beta_{gh}E_{gh}$, we find that

$$\beta_{gh} \;=\; (1 - \frac{1}{2}\delta_{gh})\frac{N_g C_{gh}}{E_{gh}}. \tag{A.9}$$

For baseline age contact matrix C_{gh}, we use the one in Table 7, obtained from Finland 2006 POLY-MOD matrix, then pairwise degree corrected, then extrapolated and density corrected, then time-corrected to represent an nonnormalised age-based contact structure in Finland in 2021 (assuming no pandemic), see [3].

A.5.1 Proof of (A.8)

For $g \neq h$ we find that $\hat{E}_{gh}^{(m)} = \hat{N}_{mg}\hat{N}_{mh}$ with the terms on the right given by (A.6). For $g = h$, we note that $\hat{E}_{gg}^{(m)} = \mathbb{E}Y_{gg}^{(m)}$ is the expectation of a random integer

$$Y_{gg}^{(m)} \;=\; \sum_{k=1}^{K}\sum_{1 \leq i < j \leq N_{kg}} B_{ki}B_{kj} \;+\; \sum_{1 \leq k < \ell \leq K}\sum_{i=1}^{N_{kg}}\sum_{j=1}^{N_{\ell g}} B_{ki}B_{\ell j},$$

where the random variables $B_{ki} \in \{0,1\}$ on the right are mutually independent and such that $\mathbb{E}B_{ki} = \theta_{km}$ for all k, i. Then a direct computation shows that

$$\begin{aligned}
\mathbb{E}Y_{gg}^{(m)} \;&=\; \sum_{k}\binom{N_{kg}}{2}\theta_{km}^2 + \frac{1}{2}\sum_{k}\sum_{\ell \neq k}N_{kg}\theta_{km}N_{\ell g}\theta_{\ell m} \\
&=\; \sum_{k}\binom{N_{kg}}{2}\theta_{km}^2 + \frac{1}{2}\left(\sum_{k}\sum_{\ell}N_{kg}\theta_{km}\right)^2 - \sum_{k}N_{kg}^2\theta_{km}^2 \\
&=\; \frac{1}{2}\hat{N}_{mg}^2 - \sum_{k}N_{kg}\theta_{km}^2.
\end{aligned}$$

B Heuristic vaccination strategies

We first analyse the different heuristic vaccination strategies to asses their impact on the development of the epidemic. Specifically, we construct different scenarios that determine the number of vaccines $v_k(t)$ that each region k will receive on day t depending on the number of infections and/or hospitalizations. Then, the vaccines $v_k(t)$ are distributed within the region in an age-prioritized strategy from old to younger age groups. We can obtain $v_k(t)$ in the following way

$$v_k(t) = v(t)\left(w_1\frac{N_k}{\sum_k N_k} + w_2\frac{I_k^D(t)}{\sum_k I_k^D(t)} + w_3\frac{H_k^D(t)}{\sum_k H_k^D(t)}\right),$$

where $v(t)$ is the overall national number of available vaccine doses on day t, w_1, w_2, and w_3 are tunable weight parameters of the strategy ($\sum_i w_i = 1$), $I_k^D(t)$ is the number of new infections, and $H_k^D(t)$ is the number hospitalized individuals in region k over the last D days. In our work we set $D = 14$ to capture the changes over two weeks starting from the initial date. The total number of

18

new infections in region k in the last D days is computed by

$$I_k^D(t) = \sum_{d=0}^{D} \sum_{g} \frac{1}{T_E} E_{kg}(t-d),$$

and similarly the number of hospitalized individuals is computed by

$$H_k^D(t) = \sum_{d=0}^{D} \sum_{g} \Big(H_{kg}^w(t-d) + H_{kg}^c(t-d) + H_{kg}^r(t-d) \Big).$$

Different vaccination strategies can be obtained by changing the weights w_i, e.g. setting $w_1 = 1$ and $w_2 = w_3 = 0$ corresponds to the baseline strategy Pop where vaccines are equally distributed according to the population density. In total we studied eight heuristic vaccination strategies with weights given in Table 2.

C Optimal control formulation

We formulate an optimal control problem with the aim of minimizing the cumulative number of deaths while satisfying the constraints of the daily maximum amount of vaccines available. More specifically, our objective is to determine optimal time-varying-per-capita rate of vaccines $\nu_{kg}(t)$ that minimizes the cumulative number of deaths calculated by (A.1). Thus, the objective functional to be minimized is given by

$$J(\nu_{kg}(t)) = \int_0^{T_f} \sum_{k=1}^{K} \sum_{g=1}^{G} D_{kg}(t)dt. \tag{C.1}$$

The optimal control formulation is: find $\nu_{kg}^*(t)$ such that

$$
\begin{aligned}
J(\nu_{kg}^*(t)) = \min_{\nu_{kg}(t)} J(\nu_{kg}(t)) \ \ \text{subject to (A.1) and} \\
\sum_{k=1}^{K} \sum_{g=1}^{G} \nu_{kg}(t) S_{kg}(t) = \nu_{\max},
\end{aligned}
\tag{C.2}
$$

where $\nu_{\max}$ is the maximum number of available vaccines per day. To solve numerically the above optimal control problem, we follow the direct discretization approach [5], that is we first discretize problem (C.2) and then solve a finite dimensional nonlinear optimization problem (NLP). We use the Pontryagin's Maximum Principle [18] to calculate the gradient with respect to the minimization variable $\nu_{kg}(t)$ that is required for the implementation of the NLP problem. This principle converts

problem (C.2) into the problem of minimizing the Hamiltonian $\mathcal{H} = \sum_{k=1}^{K} \sum_{g=1}^{G} \mathcal{H}_{kg}$ given by

$$
\begin{aligned}
\mathcal{H}_{kg} \;=\; & D_{kg} \\
& + \Lambda_{S_{kg}^u}\left(-\lambda_{kg} S_{kg}^u - v_{kg} S_{kg}^u\right) \\
& + \Lambda_{S_{kg}^v}\left(v_{kg} S_{kg}^u - \lambda_{kg}(t) S_{kg}^v - \frac{1}{T_V} S_{kg}^v\right) \\
& + \Lambda_{S_{kg}^x}\left((1-\alpha e)\frac{1}{T_V} S_{kg}^v - \lambda_{kg} S_{kg}^x\right) \\
& + \Lambda_{E_{kg}}(t)\left(\lambda_{kg}(S_{kg}^u + S_{kg}^v(t) + S_{kg}^x) - \frac{1}{T_E} E_{kg}\right) \\
& + \Lambda_{I_{kg}}\left(\frac{1}{T_E} E_{kg} - \frac{1}{T_I} I_{kg}\right) \\
& + \Lambda_{Q_{kg}^0}\left((1-p_g^h)\frac{1}{T_I} I_{kg} - \frac{1}{T_{Q^0}} Q_{kg}^0\right) \\
& + \Lambda_{Q_{kg}^1}\left(p_g^h \frac{1}{T_I} I_{kg} - \frac{1}{T_{Q^1}} Q_{kg}^1\right) \qquad\qquad\text{(C.3)} \\
& + \Lambda_{H_{kg}^w}(t)\left(\frac{1}{T_{Q^1}} Q_{kg}^1(t) - \frac{1}{T_{H^w}} H_{kg}^w(t)\right) \\
& + \Lambda_{H_{kg}^c}\left(p_g^c \frac{1}{T_{H^w}} H_{kg}^w - \frac{1}{T_{H^c}} H_{kg}^c\right) \\
& + \Lambda_{H_{kg}^r}\left((1-\mu_g^c)\frac{1}{T_{H^c}} H_{kg}^c - \frac{1}{T_{H^r}} H_{kg}^r\right) \\
& + \Lambda_{R_{kg}}\left((1-\mu_g^q)\frac{1}{T_{Q^0}} Q_{kg}^0 + (1-\mu_g^w)(1-p_g^c)\frac{1}{T_{H^w}} H_{kg}^w + \frac{1}{T_{H^r}} H_{kg}^r\right) \\
& + \Lambda_{D_{kg}}\left(\mu_g \frac{1}{T_{Q^0}} Q_{kg}^0 + \mu_g^w(1-p_g^c)\frac{1}{T_{H^w}} H_{kg}^w + \mu_g^c \frac{1}{T_{H^c}} H_{kg}^c\right) \\
& + \Lambda_{V_{kg}}\left(\alpha e \frac{1}{T_V} S_{kg}^v\right),
\end{aligned}
$$

where $\Lambda_X, X \in \{S_{kg}^u, S_{kg}^v, S_{kg}^x, E_{kg}, I_{kg}, Q_{kg}^0, Q_{kg}^1, H_{kg}^w, H_{kg}^c, H_{kg}^r, R_{kg}, D_{kg}, V_{kg}\}$ are the Lagrange multipliers [5]. Then, we differentiate $\mathcal{H}$ with respect to $\nu_{kg}(t)$ to obtain

$$
\frac{\partial \mathcal{H}}{\partial \nu_{kg}} \;=\; -\left(\Lambda_{S_{kg}^u}(t) - \Lambda_{S_{kg}^v}(t)\right) S_{kg}^u(t).
$$

Further, we differentiate $\mathcal{H}$ with respect to the state variables $S_{kg}^u, S_{kg}^v, S_{kg}^x, E_{kg}, I_{kg}, Q_{kg}^0, Q_{kg}^1, H_{kg}^w,$ $H_{kg}^c, H_{kg}^r, R_{kg}, D_{kg}, V_{kg}$ to derive the so-called adjoint system of equations. Letting $\Lambda_Y = [\Lambda_{S_{kg}^u}, \Lambda_{S_{kg}^v}, \Lambda_{S_{kg}^x},$ $\Lambda_{E_{kg}}, \Lambda_{I_{kg}}, \Lambda_{Q_{kg}^0}, \Lambda_{Q_{kg}^1}, \Lambda_{H_{kg}^w}, \Lambda_{H_{kg}^c}, \Lambda_{H_{kg}^r}, \Lambda_{R_{kg}}, \Lambda_{D_{kg}}, \Lambda_{V_{kg}}]$ and $Y = [S_{kg}^u, S_{kg}^v, S_{kg}^x, E_{kg}, I_{kg}, Q_{kg}^0, Q_{kg}^1, H_{kg}^w,$ $H_{kg}^c, H_{kg}^r, R_{kg}, D_{kg}, V_{kg}]$, we have

$$
\dot{\Lambda}_Y(t) = -\frac{\partial \mathcal{H}}{\partial Y},
$$

with the transversality conditions

$$
\Lambda_Y(T) = 0.
$$

We solve the adjoint system of equations backwards in time since we only have the final conditions.

D   Data and parameters

D.1   Disease transmission and severity parameters

Key epidemic parameters are described in Table 5.

	Description	0–9	10–19	20–29	30–39	40–49	50–59	60–69	70–79	80+
T_E	Latent period	3	3	3	3	3	3	3	3	3
T_I	Transmission period	4	4	4	4	4	4	4	4	4
$T_{Q}0$	Quarantine period (mild)	5	5	5	5	5	5	5	5	5
$T_{Q}1$	Quarantine period (severe)	3	3	3	3	3	3	3	3	3
$T_H w$	Hospital ward period	5	5	5	5	5	5	5	5	5
$T_H c$	Critical care period	9	9	9	9	9	9	9	9	9
$T_H r$	Post-critical care period	1	1	1	1	1	1	1	1	1
T_V	Vaccination immunity delay	10	10	10	10	10	10	10	10	10
p_g^h	Fraction of severe cases	0	0	0.02	0.03	0.04	0.08	0.16	0.43	0.52
p_g^c	Fraction of critical cases among severe	0	0	0	0	0	0.01	0.03	0.05	0.01
μ_g^q	Mortality, quarantine	0	0	0	0	0	0	0	0.08	0.2
μ_g^h	Mortality, hosp. ward	0	0	0	0	0	0	0	0.2	0.4
μ_g^c	Mortality, critical care	0.35	0.1	0.1	0.15	0.15	0.22	0.46	0.49	0.52
α	Vaccine acceptance	0.9	0.9	0.9	0.9	0.9	0.9	0.9	0.9	0.9
e	Vaccine efficacy	0.7	0.7	0.7	0.7	0.7	0.7	0.7	0.7	0.7

Table 5:   Parameters obtained from [27] except for e. The vaccine efficacy depends on several factors including vaccination type, disease variant, number of doses and time from the vaccination [19, 28, 29], and here we set the vaccine efficacy e following Ref. [25].

D.2   Demographic data for Finland

	0–9	10–19	20–29	30–39	40–49	50–59	60–69	70–79	80+	Total
HYKS	221613	238313	272674	316173	285988	289128	256006	212089	106198	2198182
TYKS	82812	93001	103572	106093	101979	111874	113383	99917	56373	869004
TAYS	88071	100864	105275	112809	106951	115157	117896	100045	55613	902681
KYS	71910	84213	92466	91390	85302	103387	119723	95591	53252	797234
OYS	80308	91471	84511	88448	82348	91225	100322	75669	42261	736563
Total	544714	607862	658498	714913	662568	710771	707330	583311	313697	5503664

Table 6:   Population size by region and age in mainland Finland on 31 Dec 2020. Obtained from [23].

D.3   Initial conditions

We obtain the initial conditions from data trying to mimic the pandemic situation in Finland as of 18 April 2021. More specifically, we calculate the initial conditions for the compartments in

	0–9	10–19	20–29	30–39	40–49	50–59	60–69	70–79	80+
0–9	4.61	1.24	0.81	1.71	1.08	0.63	0.58	0.15	0.08
10–19	1.10	7.83	0.97	1.02	1.83	0.71	0.35	0.13	0.07
20–29	0.71	0.95	3.87	1.84	1.51	1.41	0.67	0.19	0.10
30–39	1.51	1.01	1.86	3.25	2.24	1.97	1.18	0.21	0.12
40–49	0.82	1.57	1.33	1.94	3.18	2.24	1.02	0.29	0.16
50–59	0.45	0.57	1.16	1.60	2.09	2.91	1.71	0.26	0.14
60–69	0.62	0.42	0.83	1.43	1.42	2.56	2.19	0.72	0.40
70–79	0.22	0.21	0.32	0.36	0.58	0.55	1.01	1.09	0.60
80+	0.22	0.21	0.32	0.36	0.58	0.55	1.01	1.09	0.60

Table 7: Finnish age contact matrix with 9 age groups and 10y age resolution. The entry on row g and column h indicates the estimated daily number of contacts made by a typical individual in age group g to individuals in age group h [22].

	HYKS	TYKS	TAYS	KYS	OYS
HYKS	1 389 016	7 688	16 710	7 789	1 774
TYKS	11 316	518 173	14 139	562	2 870
TAYS	22 928	12 404	511 506	4 360	1 675
KYS	8 990	365	4 557	459 867	3 286
OYS	1 798	2 417	1 592	3 360	407 636

Table 8: Finnish regional morning (between 6:00–11:59) mobility, averaged over March–May 2019. Rows represent origins and columns represent destinations. (Source: Telia Crowd Insights)

(A.1)-(A.4) as follows

$$S_{kg}^u = N_{kg} - S_{kg}^v - S_{kg}^x - E_{kg} - I_{kg} - Q_{kg}^0 - Q_{kg}^1 - H_{kg}^w - H_{kg}^c - H_{kg}^r - R_{kg} - D_{kg} - V_{kg}$$
$$S_{kg}^v = 0$$
$$S_{kg}^x = (1-e)v_{kg}$$
$$E_{kg} = \frac{T_E}{T_I + T_E} i_{kg}^r$$
$$I_{kg} = \frac{T_I}{T_I + T_E} i_{kg}^r$$
$$Q_{kg}^0 = 0$$
$$Q_{kg}^1 = 0$$
$$H_{kg}^w = h_k \mathcal{H}_g$$
$$H_{kg}^c = c_k \mathcal{C}_g$$
$$H_{kg}^r = 0$$
$$R_{kg} = r_{kg}^r$$
$$D_{kg} = 0$$
$$V_{kg} = e\, v_{kg},$$

where v_{kg} is the cumulative number of people who have received the first dose of any vaccine until 18 April 2021, i_{kg}^r stands for the estimated number of real infectious, r_{kg}^r represents the number of real recovered people as of 18 April, h_k is the reported individuals in hospital ward, c_k is the

reported individuals in critical care units, and $\mathcal{H}_g$ and $\mathcal{C}_g$ are the proportions of people at ward and critical care, respectively. The estimation of real infectious individuals at any day t is derived directly from data as follows:

$$i_{kg}^r(t) = i_{kg}^d(t) + i_{kg}^u(t),$$

where the number of undetected infectious people $i_{kg}^u(t)$ come from upscaling the number of detected individuals $i_{kg}^d(t)$ by a factor that depends on the index of age group g, i.e.,

$$i_{kg}^u(t) = (1 + 9g^{-2.46})i_{kg}^d(t).$$

The number of detected infectious people is calculated by summing the reported cases over the last $T_I + T_E$ days,

$$i_{kg}^d(t) = \sum_{\omega=\omega_0}^{t} i_k^d(\omega)\mathcal{I}_g^w(\omega),$$

where $\omega_0 = t - T_I - T_E$, $i_k^d(t)$ is the number of cases in region k reported by THL (Finnish Institute of Health and Welfare) at day t, and $\mathcal{I}_g^w(t)$ is the proportion of infected people in age group g. We do not have daily counts as THL does not provide these on infected people per age group. We have chosen 18 April 2021 as the start day since it is a Sunday, and the weekly proportion $\mathcal{I}_g^w(t)$ is the same for all the sums ($T_I + T_E = 7$ days, 1 week), which gives

$$i_{kg}^d(t) = \mathcal{I}_g^w \sum_{\omega=\omega_0}^{t} i_k^d(\omega).$$

The numerical value for $\mathcal{I}_g^w$ can be found in Table 9 and for the result of the summation $\sum_{\omega} i_k^d(\omega)$ see Table 10. The estimation of real recovered people at day t is similar,

$$r_{kg}^r(t) = r_{kg}^d(t) + r_{kg}^u(t)$$
$$r_{kg}^u(t) = (1 + 9g^{-2.46})r_{kg}^d(t)$$
$$r_{kg}^d(t) = \sum_{\omega=0}^{t-(T_I+T_E)} i_k^d(\omega)\mathcal{I}_g^w(\omega)$$

in which $\omega = 0$ marks the beginning of the coronavirus epidemic in Finland. The estimated values at 18 April 2021 of the real infected people i_{kg}^r and real recovered people r_{kg}^r can be found in Tables 13 and 14, respectively.

Parameter	Description	0–9	10–19	20–29	30–39	40–49	50–59	60–69	70–79	80+
$\mathcal{H}_g$*	Proportion in ward	0.0058	0.0107	0.0467	0.0605	0.0911	0.1450	0.1547	0.2008	0.2847
$\mathcal{C}_g$*	Proportion in critical care	0.0038	0.0069	0.0301	0.0390	0.0978	0.2231	0.2891	0.2448	0.0655
$\mathcal{I}^w$**	Infections	240	310	354	355	294	200	101	44	31
$\mathcal{I}^w_g$	Normalized $\mathcal{I}^w$	0.1244	0.1607	0.1835	0.1840	0.1524	0.1037	0.0524	0.0228	0.0161

Table 9: Parameters for age compartments.

* From [27].

** Reported number of infected people in Finland by age group during 12–18 April 2021 [10].

Parameter	Description	HYKS	TYKS	TAYS	KYS	OYS	Total
h_k*	Ward	88	11	17	5	11	132
c_k*	Critical care	21	6	2	5	0	34
$\sum_\omega i^d_k(\omega)$**	Infectious	1179	347	225	80	76	1907

Table 10: Parameters estimated from data

* Numbers reported by [1] on 19 April 2021.

** Sum of reported number of infected people by region from 12–18 April 2021 [10].

v_{kg}	HYKS	TYKS	TAYS	KYS	OYS	Total	Total/N_g (%))
0–9	0	0	0	0	0	0	0
10–19	1802	895	647	467	397	4208	0.69
20–29	14326	6391	4806	4111	3570	33204	5.04
30–39	22284	8958	7639	6314	5640	50835	7.11
40–49	32713	12418	11718	8261	7842	72952	11.01
50–59	53123	20671	20143	15545	14676	124158	17.47
60–69	111319	46461	47329	40640	33953	279702	39.54
70–79	184419	87350	85498	79872	63631	500770	85.85
80+	94809	50321	49239	47561	37125	279055	88.96
Total	514795	233465	227019	202771	166834	1344884	24.44
Total/N_k (%)	23.42	26.87	25.15	25.43	22.65	24.44	

Table 11: Number of vaccinated people in Finland by region with 9 age groups and 10y age resolution as of 18 April 2021. The entry on row g and column k indicates the number of individuals who have received the first dose in age group g and region k. Data from [10].

S^u_{kg}	HYKS	TYKS	TAYS	KYS	OYS	Total	Total/N_g (%)
0–9	171581.02	70816.88	81903.12	67257.71	76718.73	468277.46	85.97
10–19	209955.74	85708.42	96837.14	80990.48	88887.55	562379.33	92.52
20–29	228534.80	89876.46	96665.64	85189.05	78392.50	578658.45	87.88
30–39	270855.73	91783.82	102310.14	82761.97	80860.11	628571.77	87.92
40–49	235429.06	85427.65	93018.80	75258.19	73005.88	562139.57	84.84
50–59	221934.99	88013.76	93279.21	86411.78	75323.60	564963.33	79.49
60–69	137785.90	65351.37	69714.24	78372.62	65760.56	416984.69	58.95
70–79	24360.73	11823.42	14133.96	15379.26	11743.93	77441.30	13.28
80+	8689.93	5505.76	6064.27	5424.06	4885.78	30569.80	9.75
Total	1509127.92	594307.53	653926.52	577045.10	555578.63	3889985.71	70.68
Total/N_k (%)	68.65	68.39	72.44	72.38	75.43	70.68	

Table 12: Number of susceptible people in Finland by region with 9 age groups and 10y age resolution as of 18 April 2021. The entry on row g and column k indicates the number of individuals who are susceptible in age group g and region k.

i^r_{kg}	HYKS	TYKS	TAYS	KYS	OYS	Total	Total/N_g (%)
0–9	1613.56	473.53	307.93	110.86	102.64	2608.52	0.48
10–19	688.86	202.16	131.46	47.33	43.82	1113.63	0.18
20–29	563.26	165.30	107.49	38.70	35.83	910.58	0.14
30–39	498.45	146.28	95.12	34.24	31.71	805.81	0.11
40–49	390.24	114.52	74.47	26.81	24.82	630.87	0.10
50–59	257.88	75.68	49.21	17.72	16.40	416.90	0.06
60–69	128.09	37.59	24.45	8.80	8.15	207.08	0.03
70–79	55.24	16.21	10.54	3.80	3.51	89.30	0.02
80+	38.66	11.35	7.38	2.66	2.46	62.50	0.02
Total	4234.25	1242.62	808.06	290.90	269.35	6845.19	0.12
Total/N_k (%)	0.19	0.14	0.09	0.04	0.04	0.12	

Table 13: Estimated number of real infectious people in Finland by region with 9 age groups and 10y age resolution as of 18 April 2021. The entry on row g and column k indicates the number of individuals who are infectious in age group g and region k.

r^r_{kg}	HYKS	TYKS	TAYS	KYS	OYS	Total	Total/N_g (%)
0–9	48404.26	11519.76	5855.94	4539.03	3486.14	73805.15	13.55
10–19	25865.12	6195.55	3247.81	2708.32	2142.57	40159.38	6.61
20–29	29244.78	7138.85	3694.80	3127.12	2512.22	45717.78	6.94
30–39	22527.03	5203.81	2763.23	2279.31	1915.45	34688.83	4.85
40–49	17445.50	4017.41	2137.80	1755.16	1474.33	26830.20	4.05
50–59	13794.60	3110.75	1682.52	1410.74	1207.43	21206.04	2.98
60–69	6751.83	1529.35	824.89	699.27	598.56	10403.91	1.47
70–79	3231.19	723.73	398.56	333.74	288.36	4975.57	0.85
80+	2633.95	531.39	297.37	262.54	244.63	3969.89	1.27
Total	169898.27	39970.61	20902.92	17115.24	13869.71	261756.74	4.76
Total/N_k (%)	7.73	4.60	2.32	2.15	1.88	4.76	

Table 14: Estimated number of real recovered people in Finland by region with 9 age groups and 10y age resolution as of 18 April 2021. The entry on row g and column k indicates the number of individuals who are recovered in age group g and region k.

E   Additional numerical results
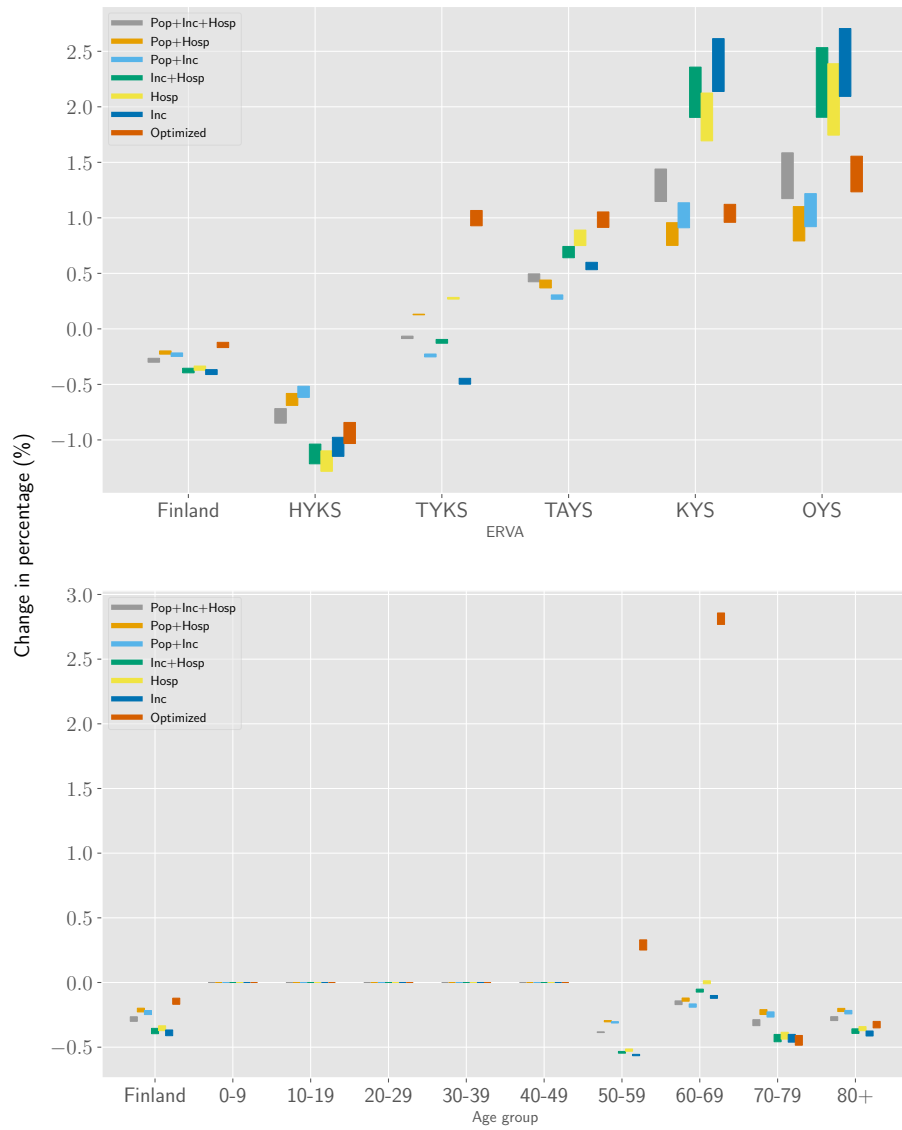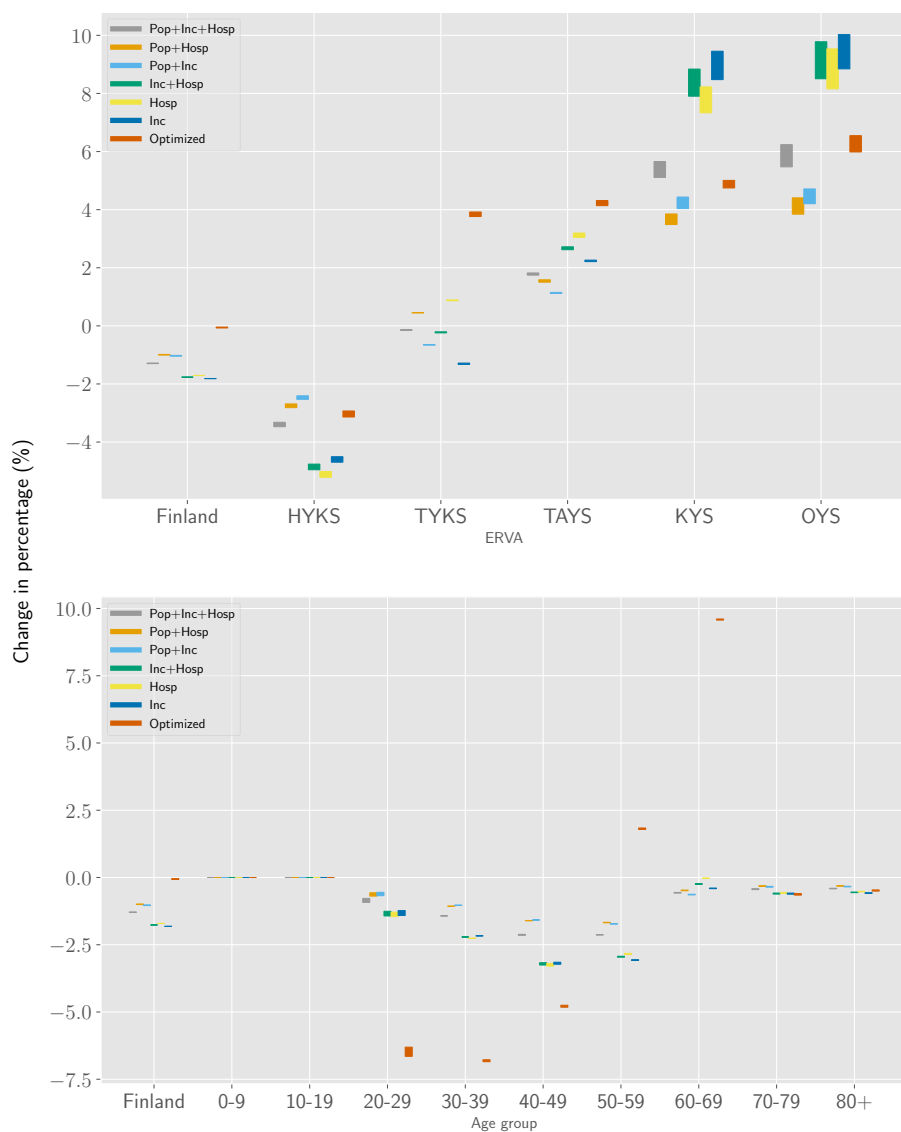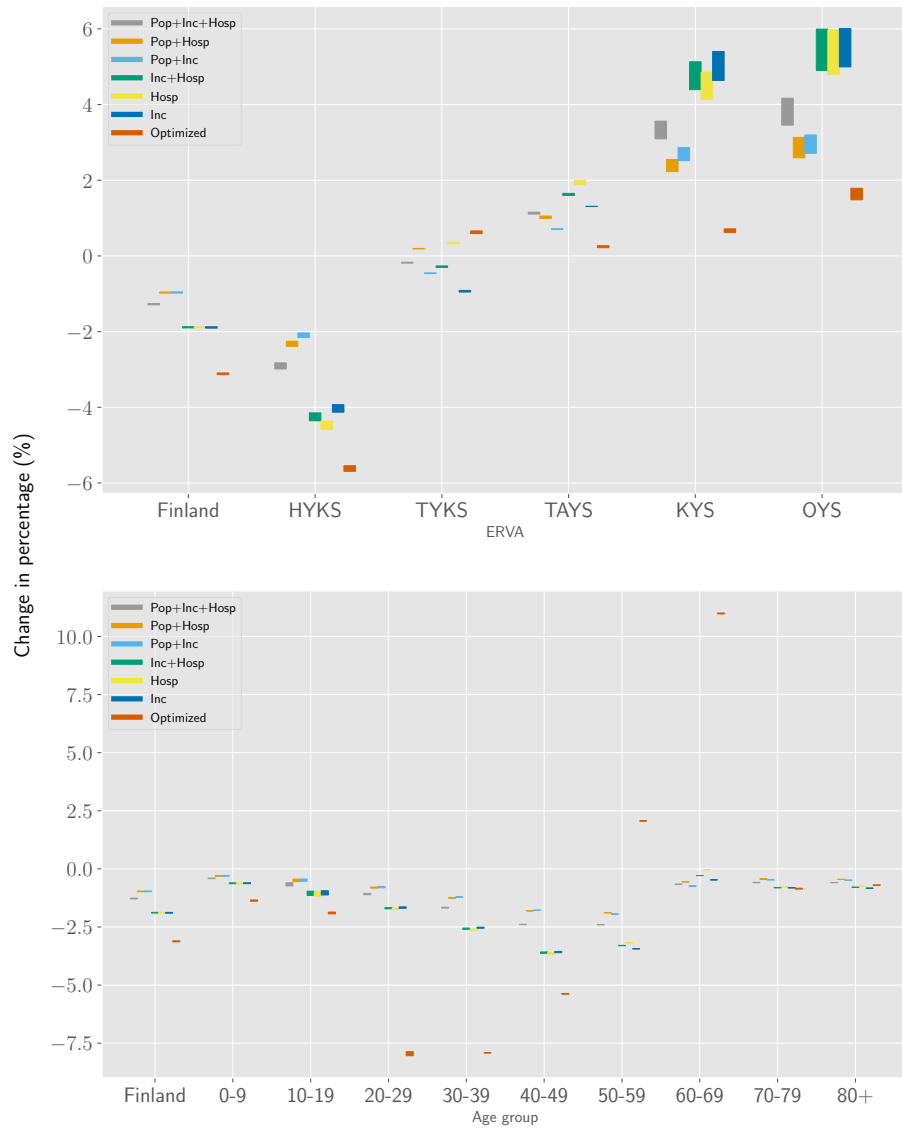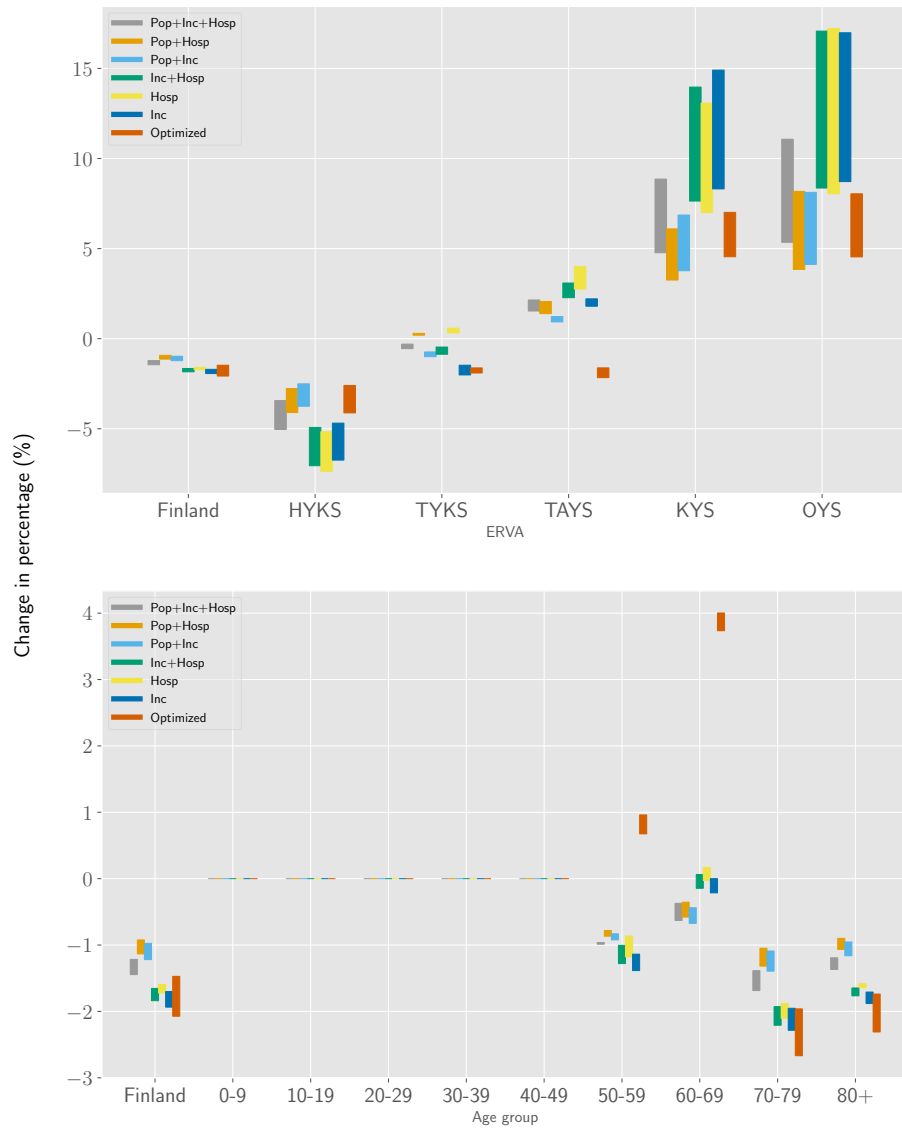
Figure 5: Relative change in mortality for all vaccination strategies with respect to the baseline strategy Pop. The bars represent the relative change in cumulative mortality between the end of the simulation and 30 days before the end of the simulation. For this scenario, the effective reproduction number $R_{\mathrm{eff}} = 0.75$ and the mobility factor $\tau = 0.5$. Top: Relative change at the regiona level. Bottom: Relative change at the age group level.
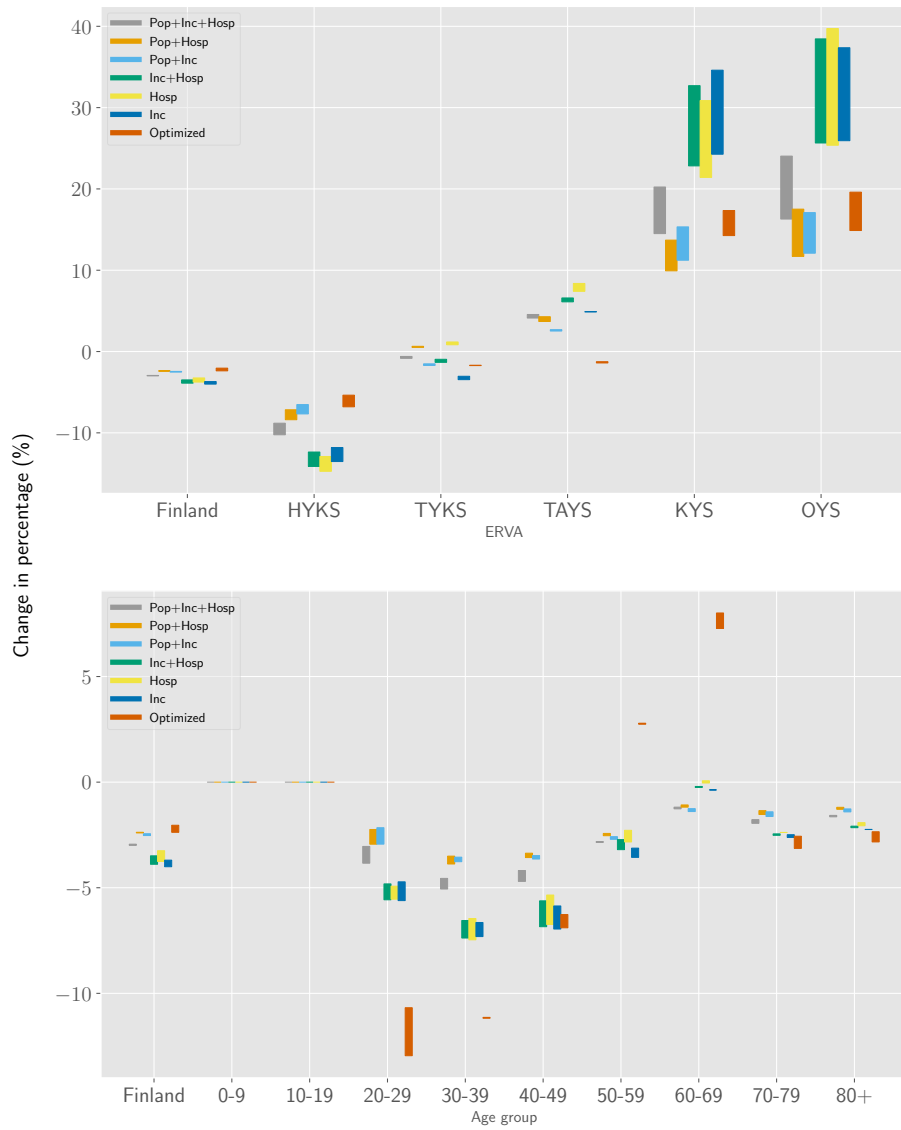
Figure 6: Relative change in new hospitalizations for all vaccination strategies with respect to the baseline strategy Pop. The bars represent the relative change in cumulative new hospitalizations between the end of the simulation and 30 days before the end of the simulation. For this scenario, the effective reproduction number $R_{\text{eff}} = 0.75$ and the mobility factor $\tau = 0.5$. Top: Relative change at the regional level. Bottom: Relative change at the age group level.
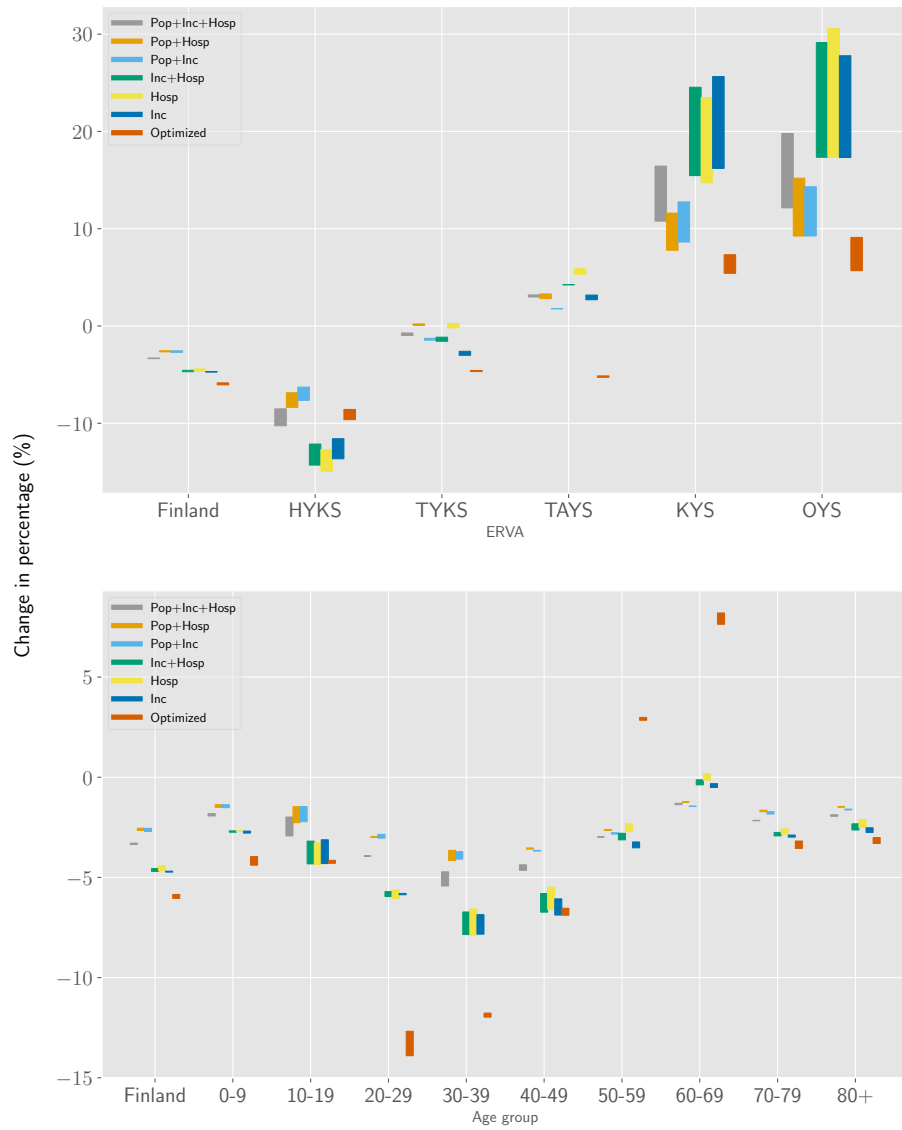
Figure 7: Relative change in incidence for all the vaccination strategies with respect to the baseline strategy Pop. The bars represent the relative change in cumulative incidence between the end of the simulation and 30 days before the end of the simulation. For this scenario, the effective reproduction number $R_{\text{eff}} = 0.75$ and the mobility factor $\tau = 0.5$. Top: Relative change at the regional level. Bottom: Relative change at the age group level.
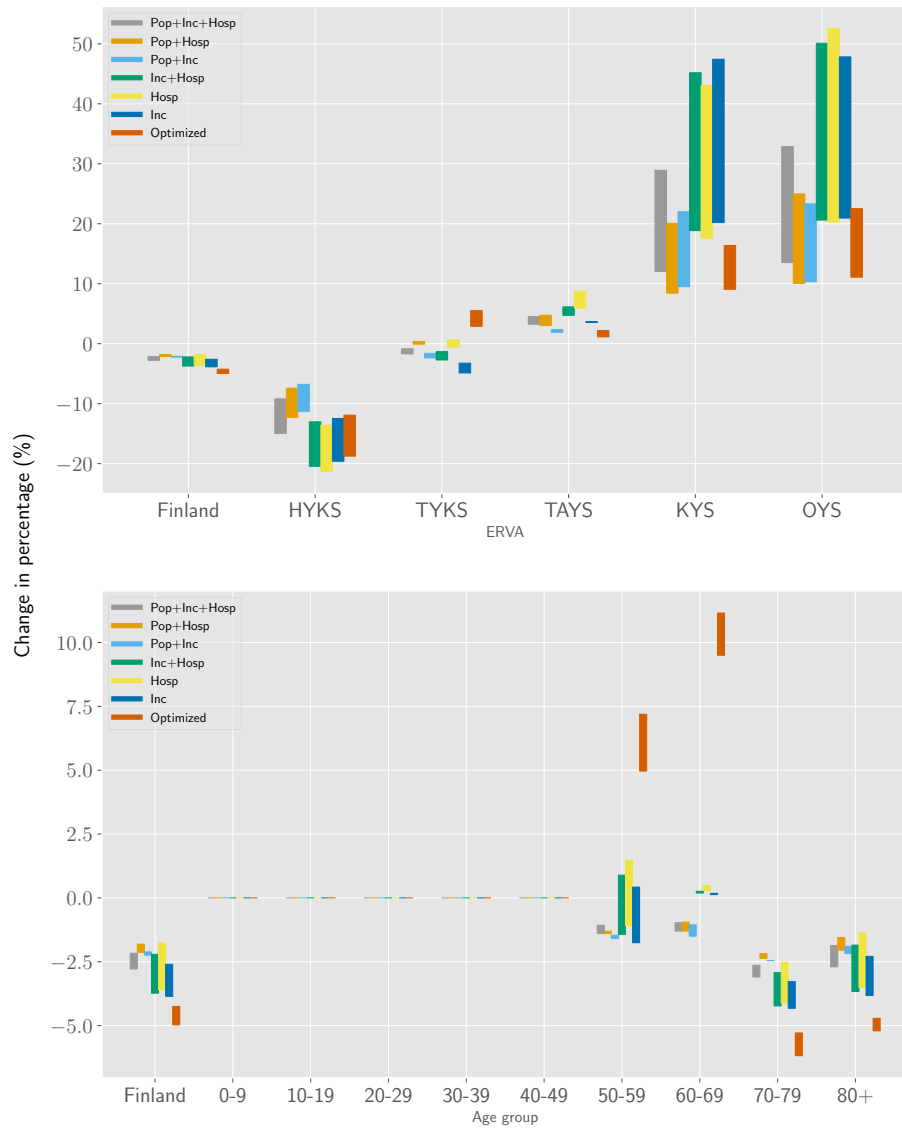
Figure 8: Relative change in mortality for all vaccination strategies with respect to the baseline strategyPop. The bars represent the relative change in cumulative mortality between the end of the simulation and 30 days before the end of the simulation. For this scenario, the effective reproduction number $R_{\text{eff}} = 1.0$ and the mobility factor $\tau = 0.5$. Top: Relative change at the regional level. Bottom: Relative change at the age group level.
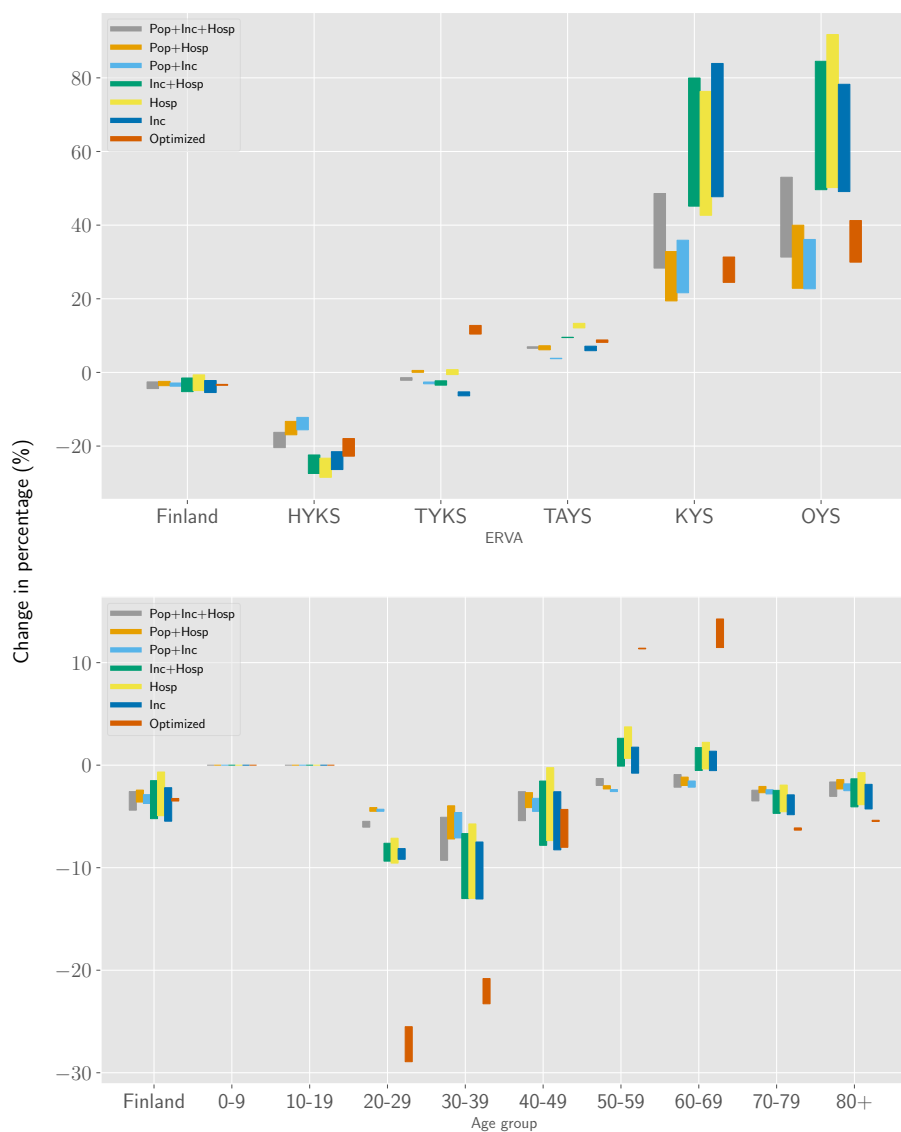
Figure 9: Relative change in new hospitalizations for all vaccination strategies with respect to the baseline strategy Pop. The bars represent the relative change in cumulative new hospitalizations between the end of the simulation and 30 days before the end of the simulation. For this scenario, the effective reproduction number $R_{\text{eff}} = 1.0$ and the mobility factor $\tau = 0.5$. Top: Relative change at the regional level. Bottom: Relative change at the age group level.

Figure 10: Relative change in incidence for all vaccination strategies with respect to the vaccination strategy baseline Pop. The bars represent the relative change in cumulative incidence between the end of the simulation and 30 days before the end of the simulation. For this scenario, the effective reproduction number $R_{\text{eff}} = 1.0$ and the mobility factor $\tau = 0.5$. Top: Relative change at the regional level, Bottom: Relative change at the age group level.
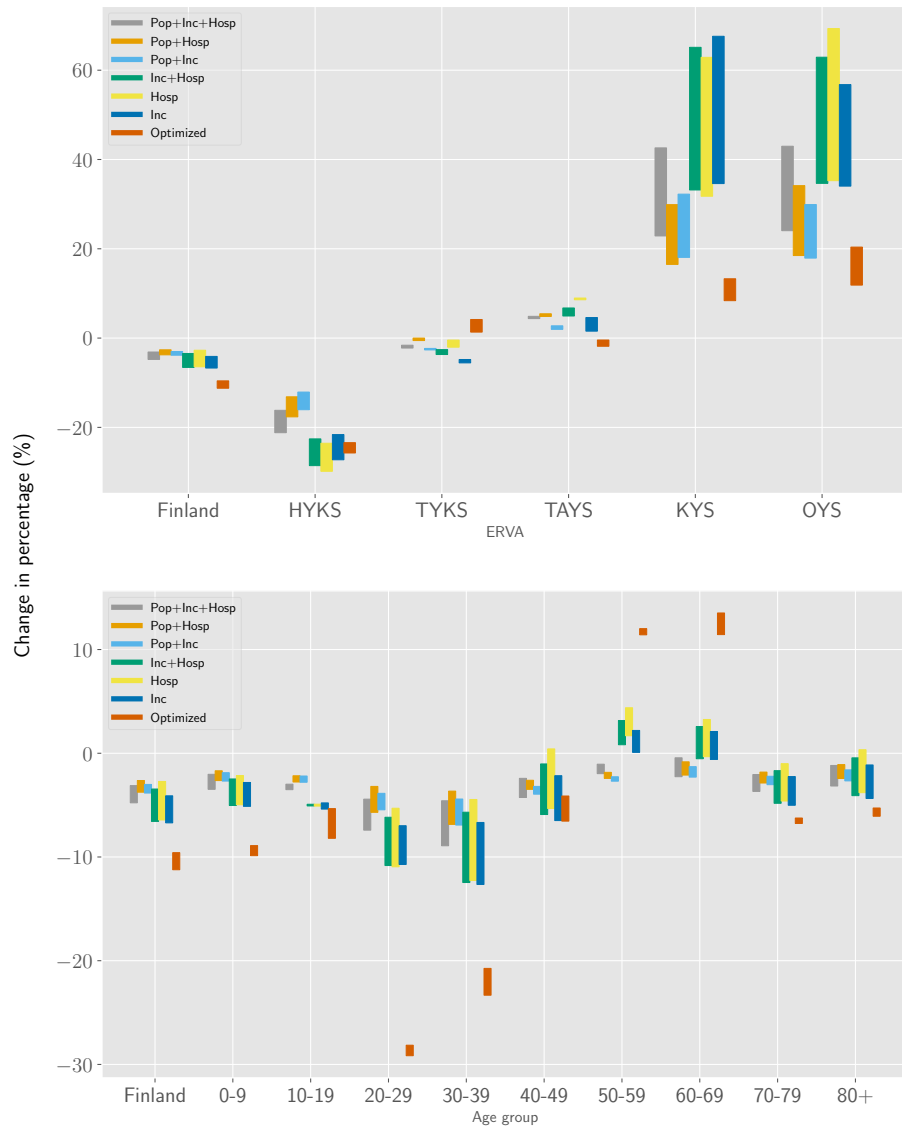
Figure 11: Relative change in mortality for all vaccination strategies with respect to the baseline strategy `Pop`. The bars represent the relative change in cumulative mortality between the end of the simulation and 30 days before the end of the simulation. For this scenario, the effective reproduction number $R_{\text{eff}} = 1.25$ and the mobility factor $\tau = 0.5$. Top: Relative change at the regional level. Bottom: Relative change at the age group level.
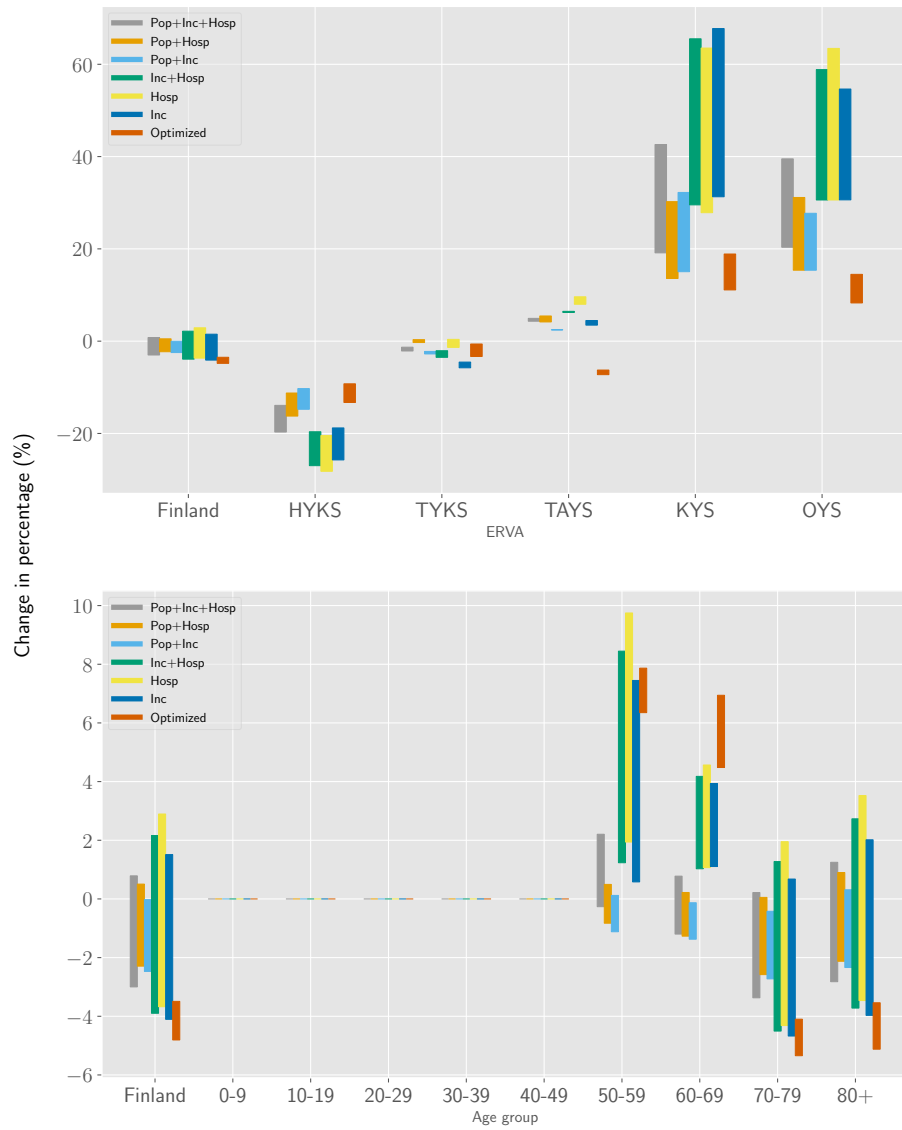
Figure 12: Relative change in new hospitalizations for all vaccination strategies with respect to the baseline strategy `Pop`. The bars represent the relative change in cumulative new hospitalizations between the end of the simulation and 30 days before the end of the simulation. For this scenario, the effective reproduction number $R_{\text{eff}} = 1.25$ and the mobility factor $\tau = 0.5$. Top: Relative change at the regional level. Bottom: Relative change at the age group level.

Figure 13: Relative change in incidence for all vaccination strategies with respect to the baseline strategy Pop. The bars represent the relative change in cumulative incidence between the end of the simulation and 30 days before the end of the simulation. For this scenario, the effective reproduction number $R_{\text{eff}} = 1.25$ and the mobility factor $\tau = 0.5$. Top: Relative change at the regional level. Bottom: Relative change at the age group level.
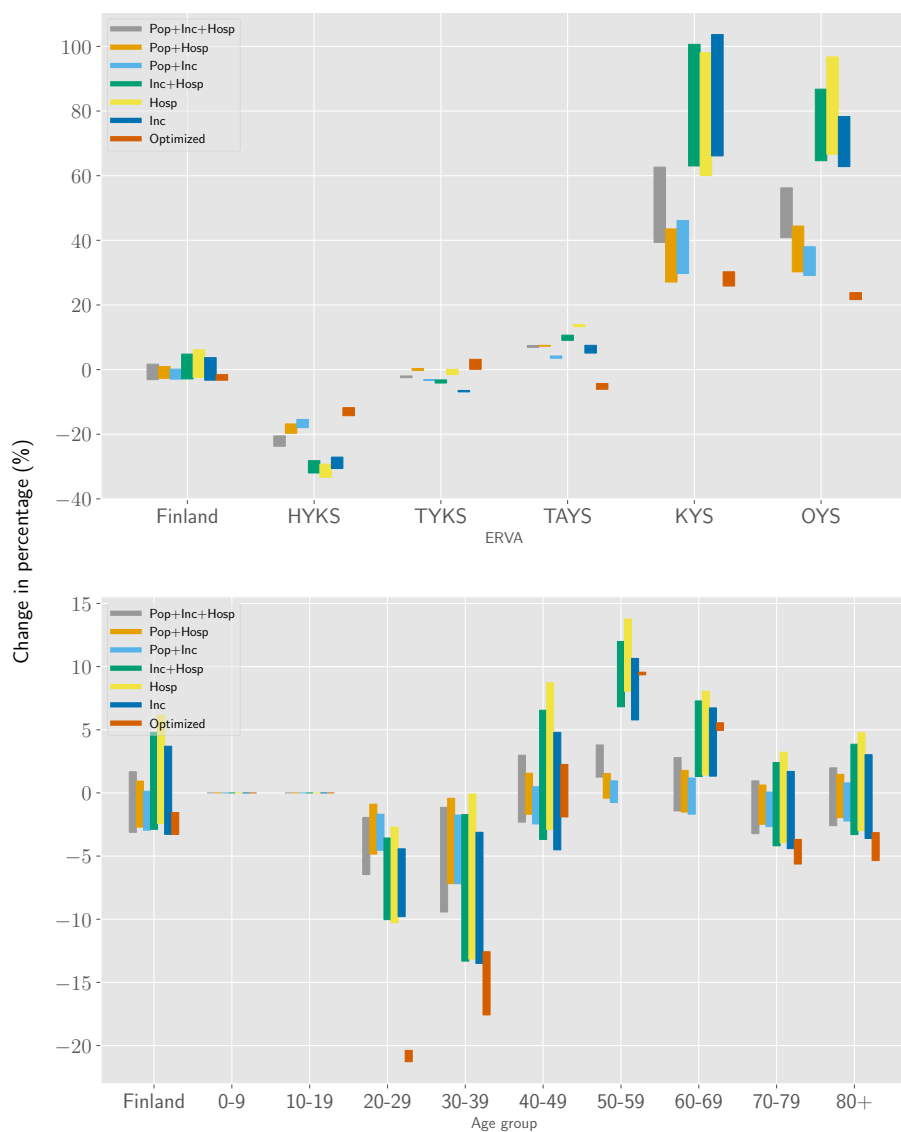
Figure 14: Relative change in mortality for all vaccination strategies with respect to the baseline strategy Pop. The bars represent the relative change in cumulative mortality between the end of the simulation and 30 days before the end of the simulation. For this scenario, the effective reproduction number $R_{\text{eff}} = 1.5$ and the mobility factor $\tau = 0.5$. Top: Relative change at the regional level. Bottom: Relative change at the age group level.
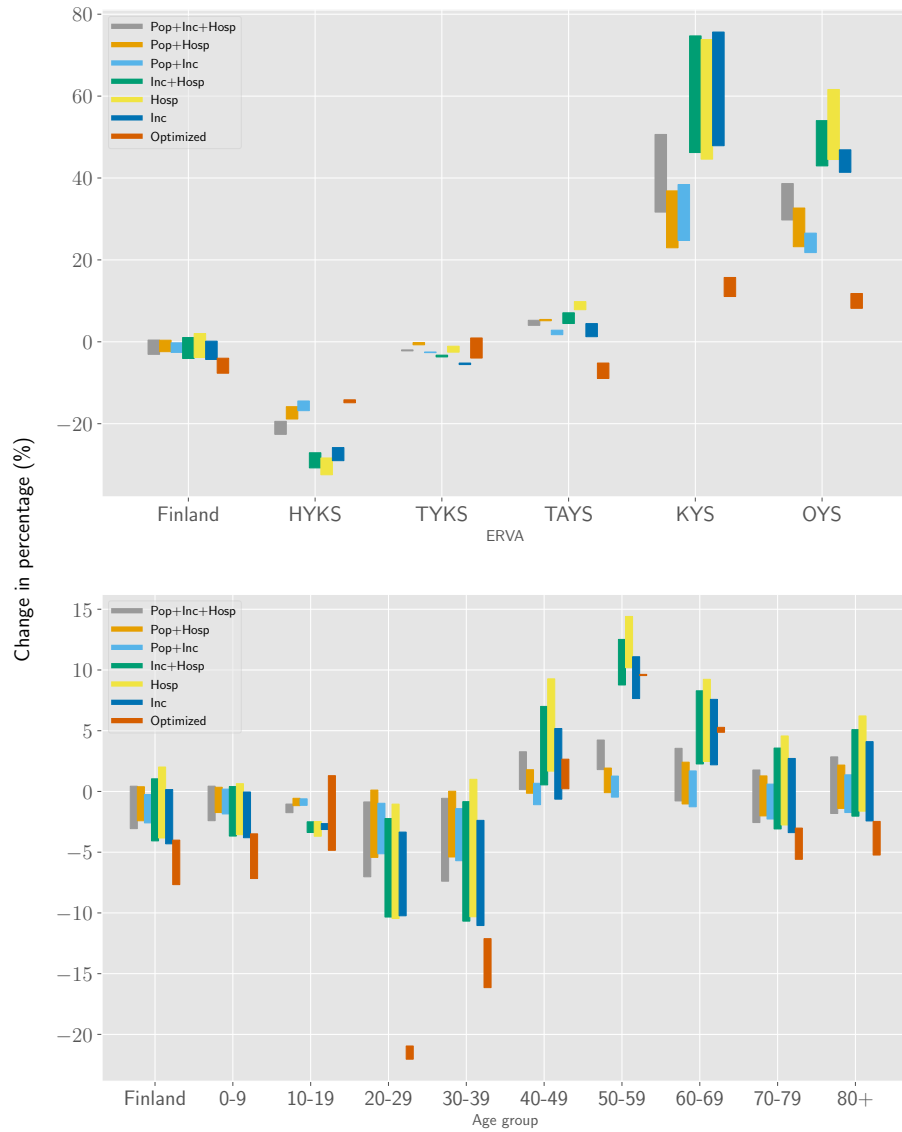
Figure 15: Relative change in new hospitalizations for all vaccination strategies with respect to the baseline strategy Pop. The bars represent the relative change in cumulative new hospitalizations between the end of the simulation and 30 days before the end of the simulation. For this scenario, the effective reproduction number $R_{\text{eff}} = 1.5$ and the mobility factor $\tau = 0.5$. Top: Relative change at the regional level. Bottom: Relative change at the age group level.

Figure 16: Relative change in incidence for all vaccination strategies with respect to the baseline strategy `Pop`. The bars represent the relative change in cumulative incidence between the end of the simulation and 30 days before the end of the simulation. For this scenario, the effective reproduction number $R_{\mathrm{eff}} = 1.5$ and the mobility factor $\tau = 0.5$. Top: relative change at the regional level. Bottom: Relative change at the age group level.

E.1 Tabulated results

	Hosp	Inc	Inc+Hosp	Pop+Hosp	Pop+Inc	Pop+Inc+Hosp	Optimized
$R_{\text{eff}} = 0.75, \tau = 0$							
Mortality	-0.24	**-0.28**	-0.26	-0.15	-0.17	-0.20	**-0.28**
New hospitalizations	-9.83	**-10.63**	-10.24	-5.75	-6.04	-7.50	0.21
Incidence	-246.71	-250.93	-248.50	-126.92	-128.37	-168.30	**-412.46**
$R_{\text{eff}} = 0.75, \tau = 0.5$							
Mortality	-0.38	**-0.42**	-0.40	-0.23	-0.25	-0.31	**-0.42**
New hospitalizations	-12.99	**-13.87**	-13.46	-7.67	-7.96	-9.91	-0.56
Incidence	-351.17	-352.77	-351.58	-181.80	-181.61	-239.02	**-580.45**
$R_{\text{eff}} = 0.75, \tau = 1$							
Mortality	-0.55	**-0.58**	-0.57	-0.32	-0.34	-0.42	**-0.58**
New hospitalizations	-16.08	**-16.82**	-16.47	-9.39	-9.58	-12.06	-1.84
Incidence	-455.96	-449.62	-452.26	-234.99	-231.05	-306.97	**-727.54**
$R_{\text{eff}} = 1.0, \tau = 0$							
Mortality	-1.59	-1.92	-1.77	-1.10	-1.24	-1.43	**-2.07**
New hospitalizations	-38.43	**-45.54**	-42.26	-28.49	-30.73	-35.37	-24.82
Incidence	-1328.43	-1479.06	-1405.00	-800.34	-842.93	-1029.51	**-2236.94**
$R_{\text{eff}} = 1.0, \tau = 0.5$							
Mortality	-3.07	-3.45	-3.27	-2.02	-2.17	-2.57	**-3.69**
New hospitalizations	-59.84	**-68.05**	-64.30	-44.32	-46.60	-54.12	-43.77
Incidence	-2308.30	-2448.11	-2381.21	-1387.21	-1415.68	-1753.48	**-3159.17**
$R_{\text{eff}} = 1.0, \tau = 1$							
Mortality	-5.61	-5.86	-5.75	-3.39	-3.48	-4.32	**-5.96**
New hospitalizations	-96.69	**-102.47**	-99.88	-65.24	-66.31	-79.95	-61.72
Incidence	-3845.06	-3859.87	-3851.98	-2209.79	-2182.09	-2783.70	**-5408.81**
$R_{\text{eff}} = 1.25, \tau = 0$							
Mortality	-1.76	-5.81	-3.90	-4.04	-5.56	-4.92	**-15.86**
New hospitalizations	7.50	-79.59	-40.55	-83.37	-111.22	-91.12	**-151.39**
Incidence	-1516.27	-4807.35	-3239.79	-2417.47	-3455.08	-3106.95	**-11834.78**
$R_{\text{eff}} = 1.25, \tau = 0.5$							
Mortality	-9.63	-14.16	-12.04	-9.86	-11.52	-11.82	**-27.10**
New hospitalizations	-43.40	-143.01	-98.29	-158.04	-186.93	-167.62	**-211.26**
Incidence	-5884.04	-8884.67	-7464.80	-5686.31	-6505.21	-6752.67	**-20750.36**
$R_{\text{eff}} = 1.25, \tau = 1$							
Mortality	-33.93	-36.55	-35.34	-22.84	-23.66	-28.12	**-47.76**
New hospitalizations	-352.81	-415.58	-387.51	-329.58	-343.41	-376.57	**-442.35**
Incidence	-19332.48	-20383.68	-19896.44	-12886.07	-12927.31	-15564.92	**-29971.58**
$R_{\text{eff}} = 1.5, \tau = 0$							
Mortality	61.95	33.41	46.81	15.29	4.11	20.52	**-46.50**
New hospitalizations	1256.84	721.48	959.43	218.51	26.79	344.51	**-203.01**
Incidence	21497.52	4323.84	12277.17	5810.86	-921.08	5905.69	**-29411.63**
$R_{\text{eff}} = 1.5, \tau = 0.5$							
Mortality	58.44	30.51	43.63	10.21	-0.47	15.88	**-70.48**
New hospitalizations	1415.30	853.04	1105.58	215.96	31.73	386.17	**-358.85**
Incidence	15340.54	1183.97	7928.77	2964.71	-1931.73	3304.50	**-30546.26**
$R_{\text{eff}} = 1.5, \tau = 1$							
Mortality	-26.50	-43.85	-35.67	-32.26	-38.48	-37.70	**-91.62**
New hospitalizations	483.83	82.09	265.57	-248.03	-364.46	-185.04	**-548.44**
Incidence	-13251.29	-20438.36	-16967.11	-11429.35	-13502.54	-13969.80	**-29973.72**

Table 15: Absolute difference in mortality, hospital load, and incidence of different vaccination policies with respect to baseline `Pop` policy. Highest reductions are indicated in bold.

	Hosp	Inc	Inc+Hosp	Pop+Hosp	Pop+Inc	Pop+Inc+Hosp	Optimized
$R_{\text{eff}} = 0.75, \tau = 0$							
Mortality	-0.25	**-0.29**	-0.27	-0.16	-0.18	-0.21	**-0.29**
New hospitalizations	-1.45	**-1.56**	-1.51	-0.85	-0.89	-1.10	0.03
Incidence	-1.53	-1.56	-1.54	-0.79	-0.80	-1.04	**-2.56**
$R_{\text{eff}} = 0.75, \tau = 0.5$							
Mortality	-0.37	**-0.41**	-0.40	-0.23	-0.25	-0.30	**-0.41**
New hospitalizations	-1.70	**-1.82**	-1.77	-1.01	-1.04	-1.30	-0.07
Incidence	-1.90	-1.91	-1.90	-0.98	-0.98	-1.29	**-3.14**
$R_{\text{eff}} = 0.75, \tau = 1$							
Mortality	-0.52	**-0.55**	-0.54	-0.30	-0.32	-0.40	**-0.55**
New hospitalizations	-1.96	**-2.05**	-2.01	-1.14	-1.17	-1.47	-0.22
Incidence	-2.26	-2.23	-2.24	-1.16	-1.14	-1.52	**-3.60**
$R_{\text{eff}} = 1.0, \tau = 0$							
Mortality	-1.06	-1.27	-1.17	-0.73	-0.82	-0.95	**-1.38**
New hospitalizations	-2.62	**-3.11**	-2.88	-1.94	-2.10	-2.41	-1.69
Incidence	-3.31	-3.69	-3.50	-2.00	-2.10	-2.57	**-5.58**
$R_{\text{eff}} = 1.0, \tau = 0.5$							
Mortality	-1.72	-1.94	-1.84	-1.13	-1.22	-1.45	**-2.07**
New hospitalizations	-3.25	**-3.69**	-3.49	-2.41	-2.53	-2.94	-2.38
Incidence	-4.42	-4.69	-4.56	-2.66	-2.71	-3.36	**-6.05**
$R_{\text{eff}} = 1.0, \tau = 1$							
Mortality	-2.81	-2.93	-2.88	-1.70	-1.74	-2.16	**-2.98**
New hospitalizations	-4.53	**-4.80**	-4.68	-3.06	-3.11	-3.75	-2.89
Incidence	-6.24	-6.26	-6.25	-3.59	-3.54	-4.52	**-8.78**
$R_{\text{eff}} = 1.25, \tau = 0$							
Mortality	-0.46	-1.52	-1.02	-1.06	-1.46	-1.29	**-4.15**
New hospitalizations	0.17	-1.77	-0.90	-1.86	-2.47	-2.03	**-3.37**
Incidence	-1.04	-3.30	-2.22	-1.66	-2.37	-2.13	**-8.12**
$R_{\text{eff}} = 1.25, \tau = 0.5$							
Mortality	-1.77	-2.60	-2.21	-1.81	-2.11	-2.17	**-4.97**
New hospitalizations	-0.67	-2.20	-1.51	-2.43	-2.87	-2.58	**-3.25**
Incidence	-2.72	-4.10	-3.45	-2.63	-3.00	-3.12	**-9.58**
$R_{\text{eff}} = 1.25, \tau = 1$							
Mortality	-5.03	-5.42	-5.24	-3.39	-3.51	-4.17	**-7.08**
New hospitalizations	-4.38	-5.16	-4.81	-4.09	-4.26	-4.67	**-5.49**
Incidence	-7.19	-7.58	-7.40	-4.79	-4.81	-5.79	**-11.14**
$R_{\text{eff}} = 1.5, \tau = 0$							
Mortality	4.53	2.45	3.43	1.12	0.30	1.50	**-3.40**
New hospitalizations	7.84	4.50	5.98	1.36	0.17	2.15	**-1.27**
Incidence	3.92	0.79	2.24	1.06	-0.17	1.08	**-5.36**
$R_{\text{eff}} = 1.5, \tau = 0.5$							
Mortality	2.90	1.51	2.16	0.51	-0.02	0.79	**-3.49**
New hospitalizations	6.14	3.70	4.79	0.94	0.14	1.67	**-1.56**
Incidence	2.01	0.16	1.04	0.39	-0.25	0.43	**-4.01**
$R_{\text{eff}} = 1.5, \tau = 1$							
Mortality	-1.09	-1.80	-1.46	-1.32	-1.58	-1.54	**-3.75**
New hospitalizations	1.76	0.30	0.97	-0.90	-1.33	-0.67	**-2.00**
Incidence	-1.51	-2.32	-1.93	-1.30	-1.53	-1.59	**-3.40**

Table 16: Relative difference in mortality, hospital load, and incidence of different vaccination policies with respect to baseline `Pop` policy. Highest reductions are indicated in bold.
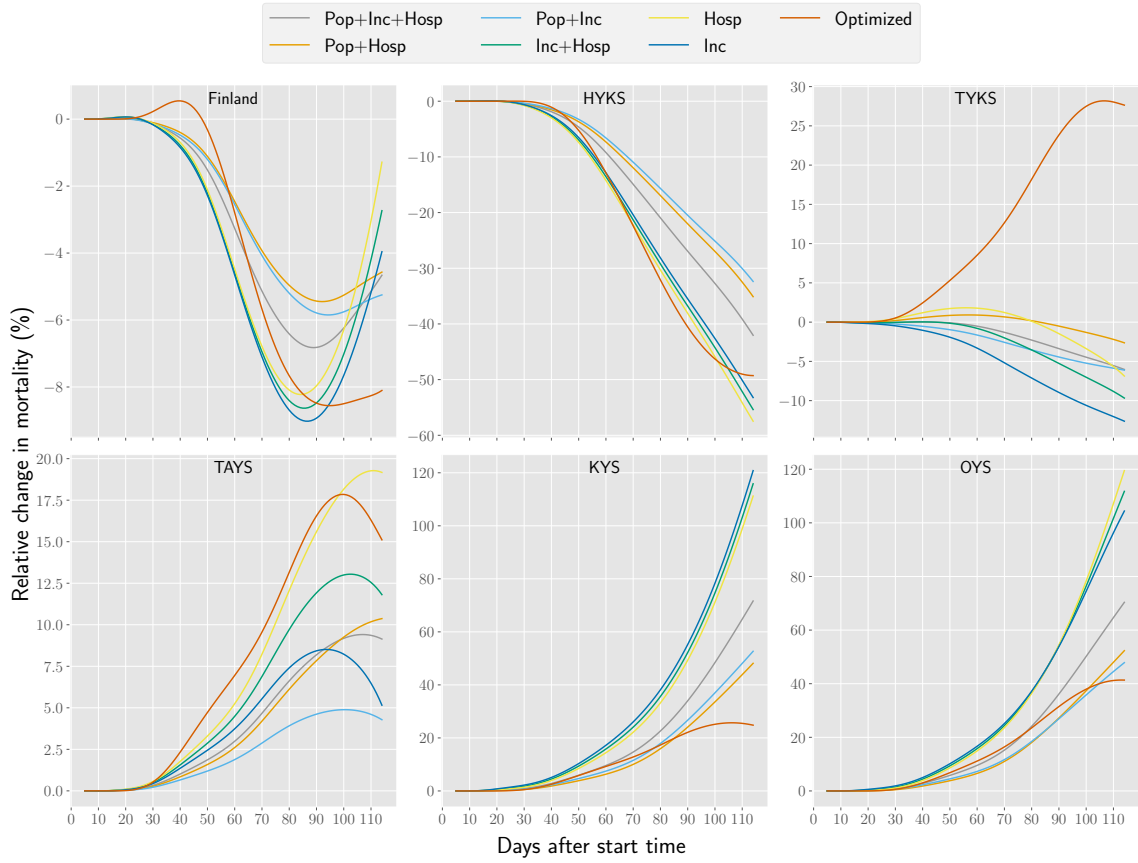
E.2   Time plots

Figure 17: Relative change in mortality for all vaccination strategies with respect to the baseline strategy `Pop`. For this scenario, the effective reproduction number $R_{\text{eff}} = 0.75$ and the mobility factor $\tau = 0.5$.
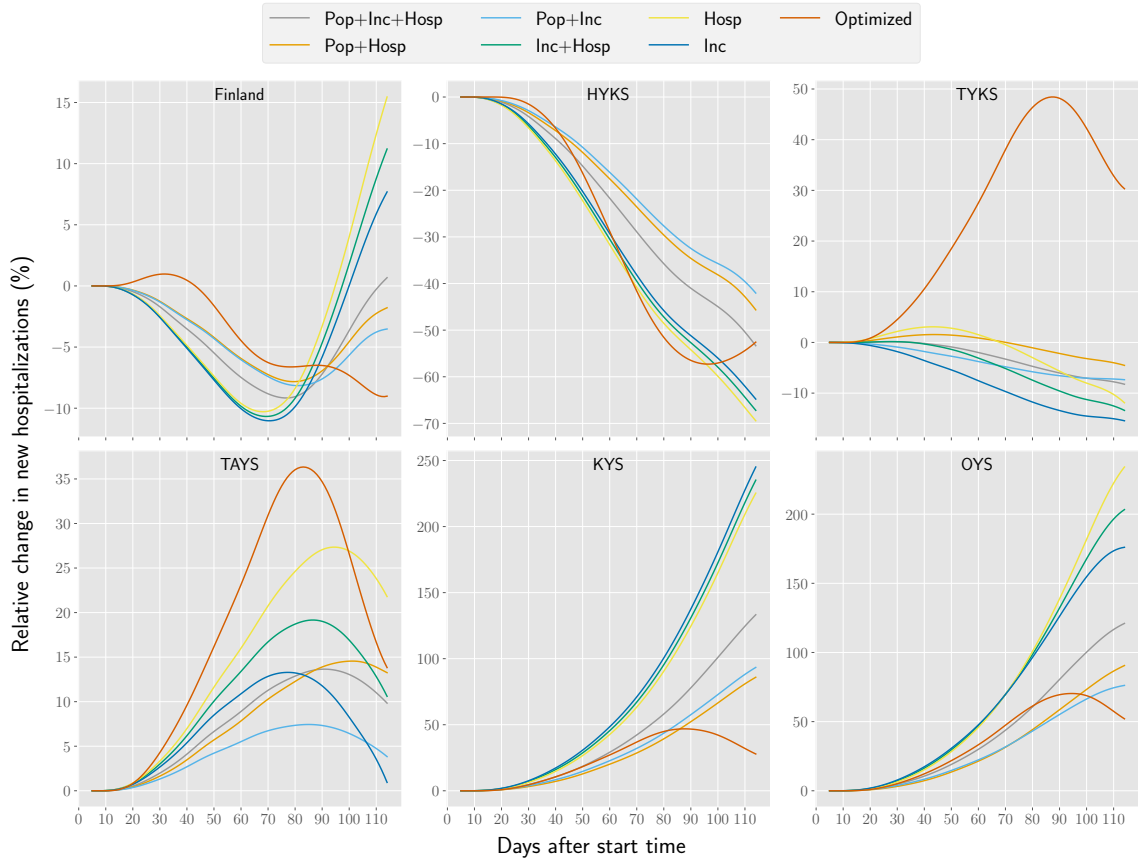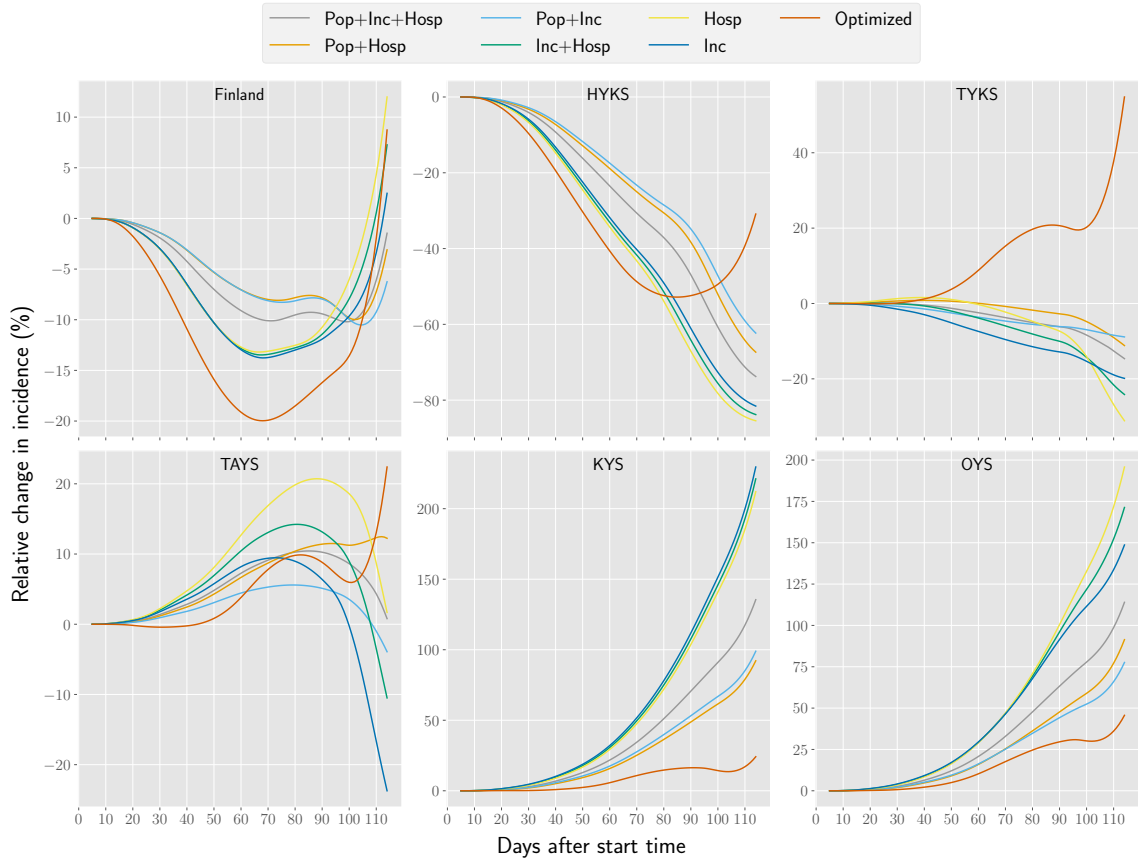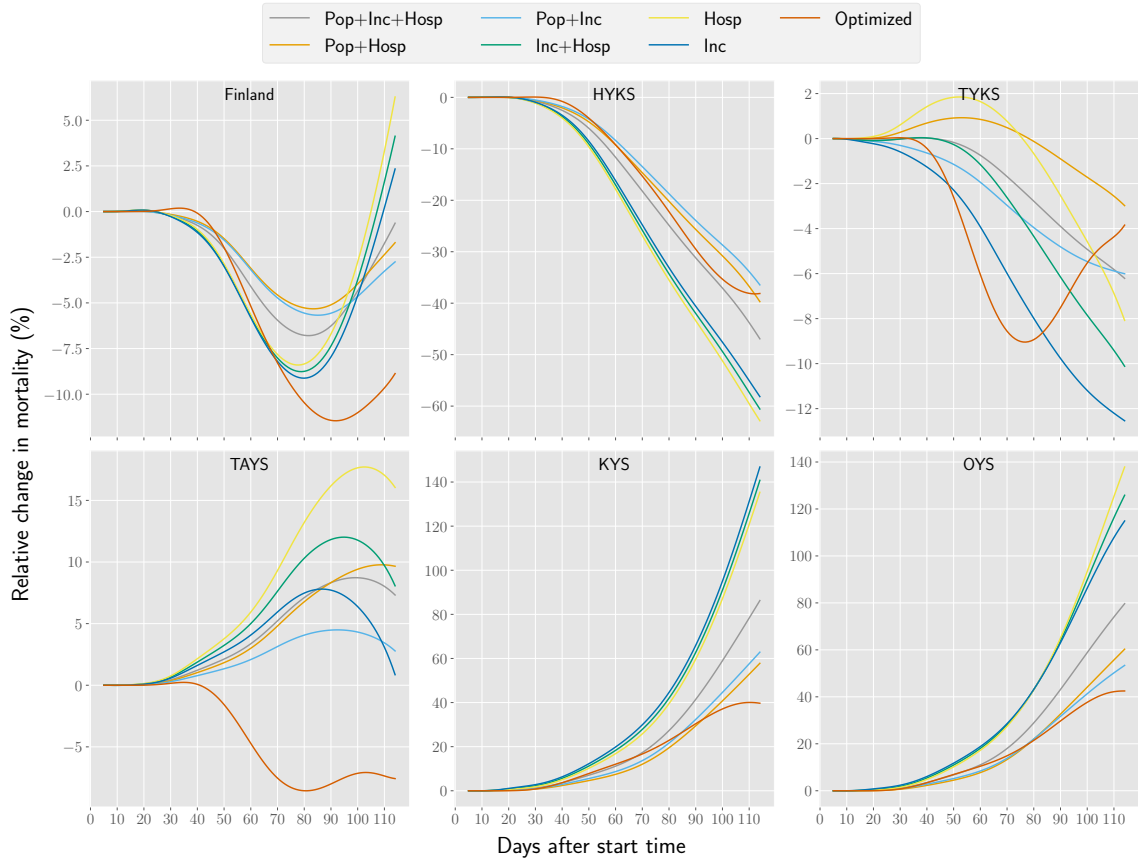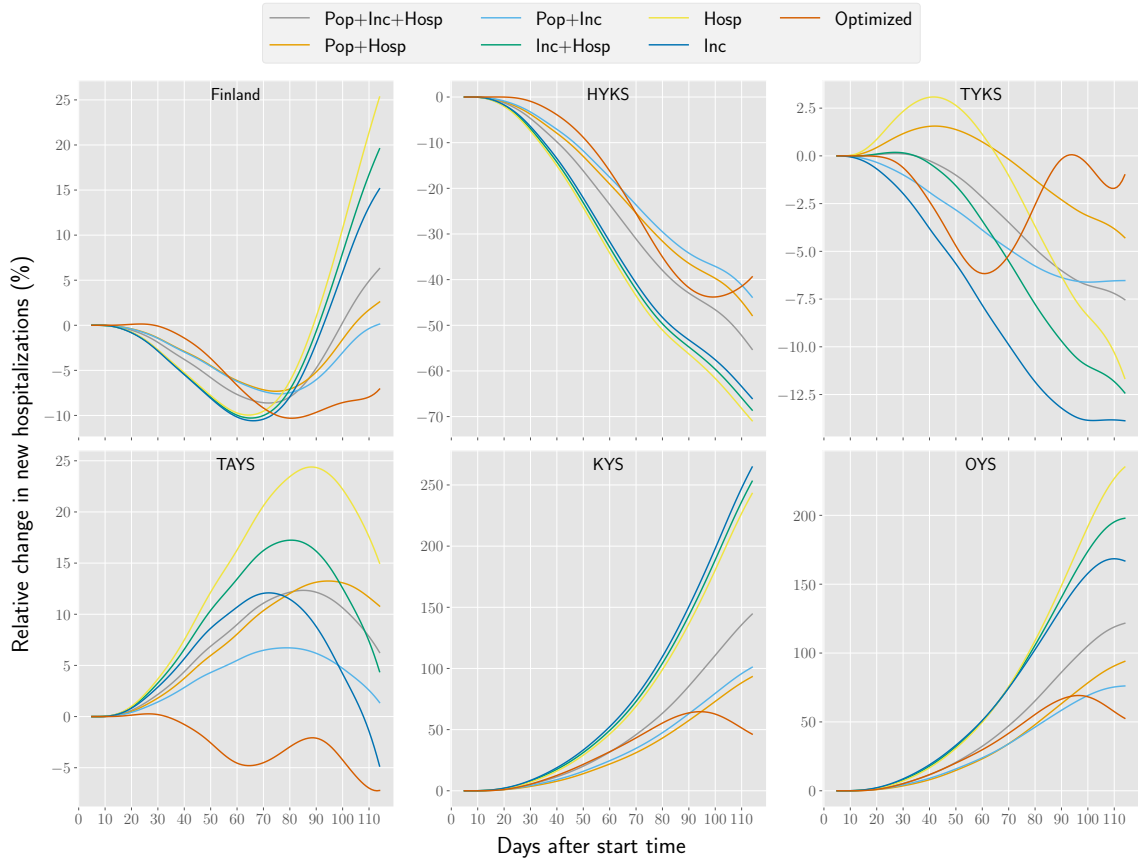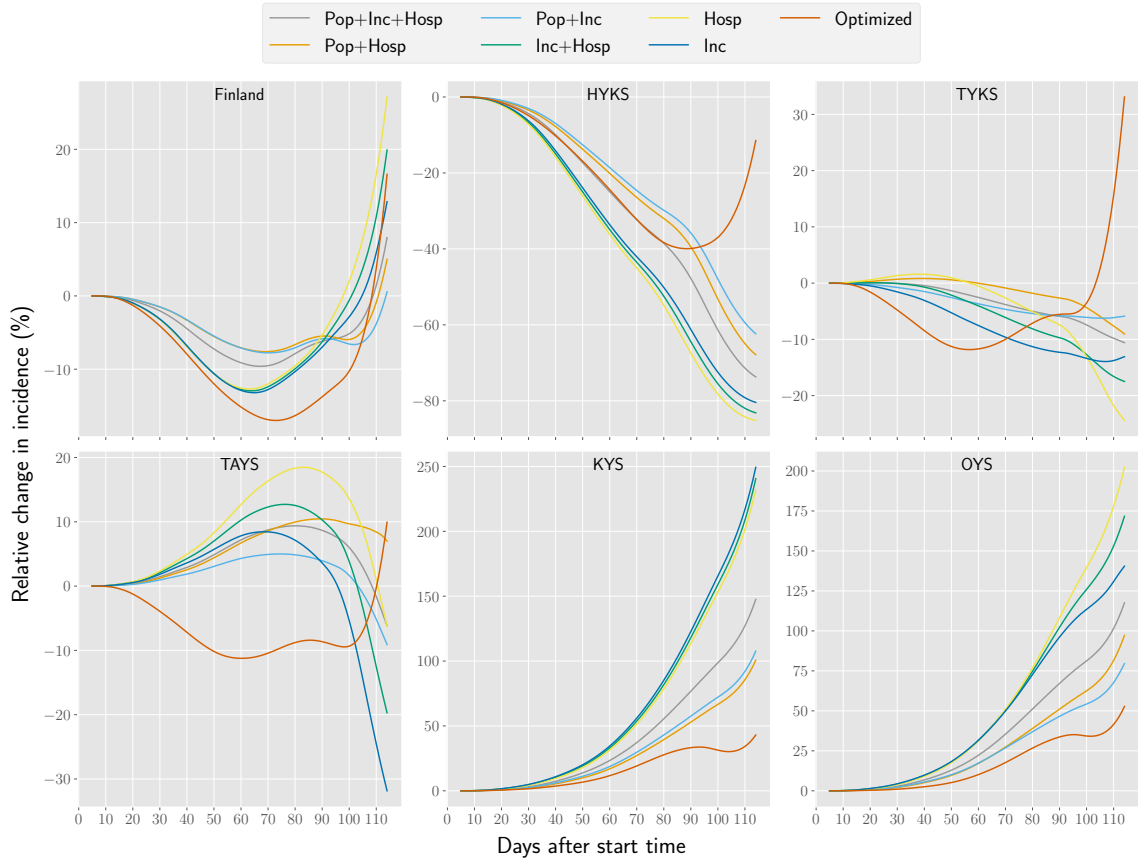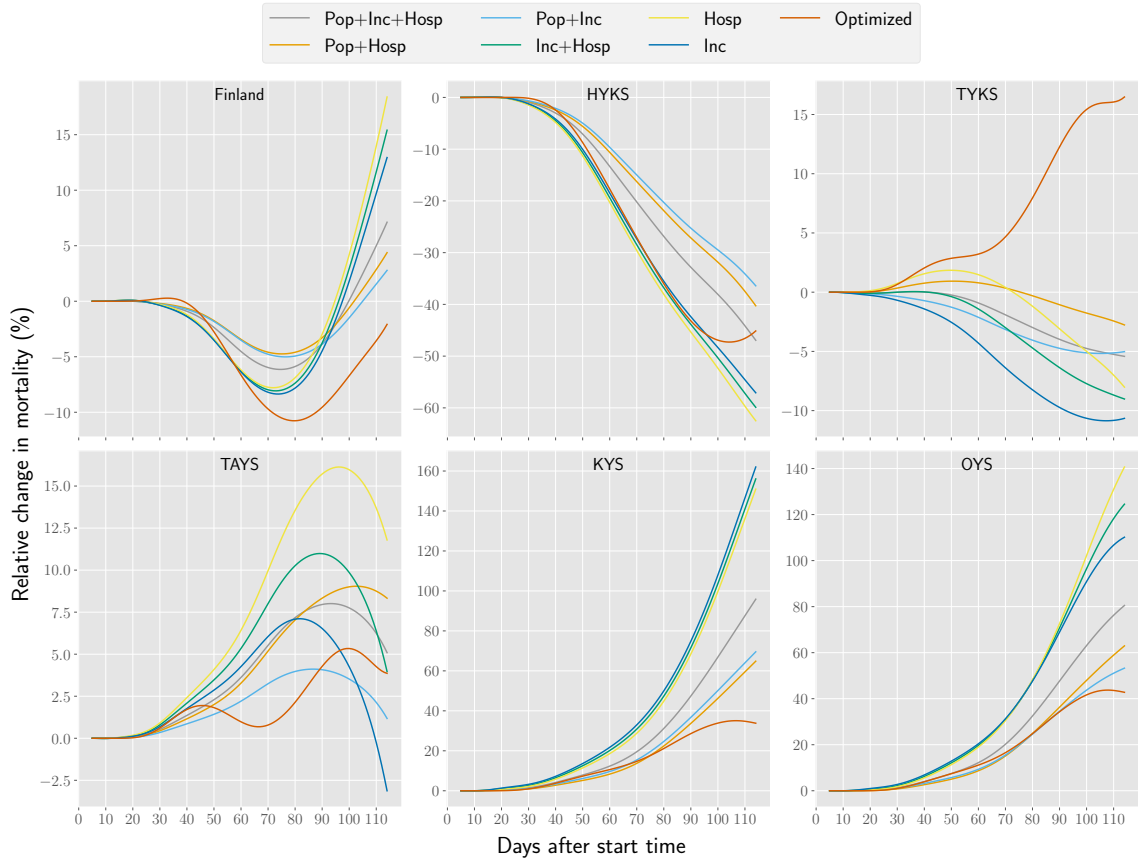
Figure 18: Relative change in new hospitalizations for all vaccination strategies with respect to vaccination strategy baseline `Pop`. For this scenario, the effective reproduction number $R_{\mathrm{eff}} = 0.75$ and the mobility factor $\tau = 0.5$.

Figure 19: Relative change in incidence for all vaccination strategies with respect to the baseline strategy `Pop`. For this scenario, the effective reproduction number $R_{\text{eff}} = 0.75$ and the mobility factor $\tau = 0.5$.

Figure 20: Relative change in mortality for all vaccination strategies with respect to the vaccination strategy baseline Pop. For this scenario, the effective reproduction number $R_{\text{eff}} = 1.0$ and the mobility factor $\tau = 0.5$.
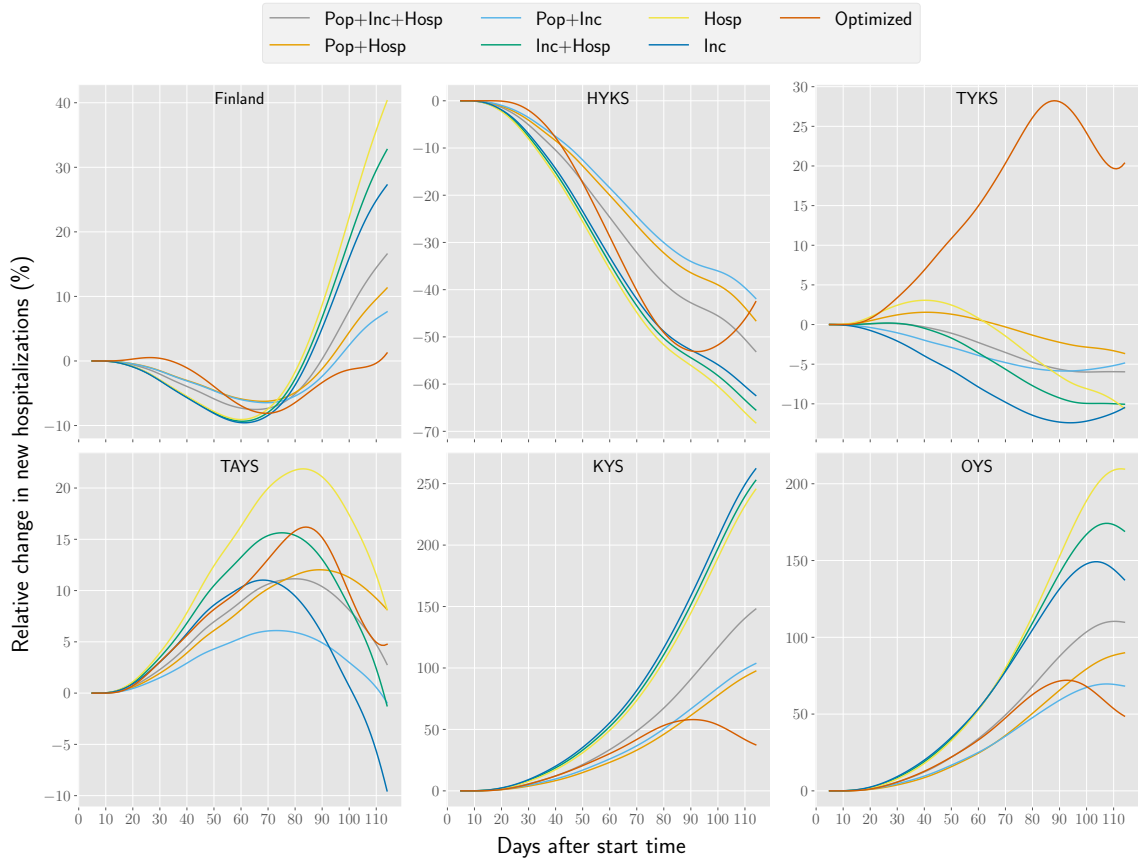
Figure 21: Relative change in new hospitalizations for all vaccination strategies with respect to the baseline strategy Pop. For this scenario, the effective reproduction number $R_{\text{eff}} = 1.0$ and the mobility factor $\tau = 0.5$.
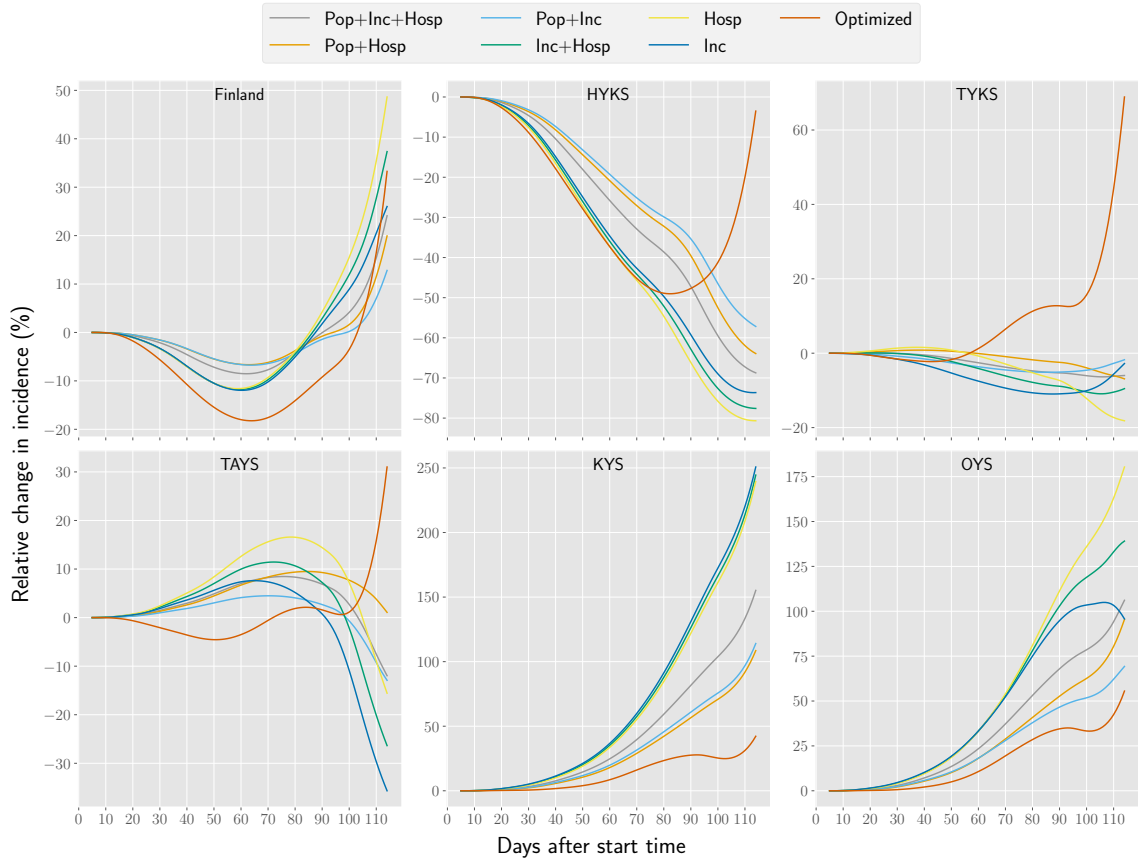
Figure 22: Relative change in incidence for all vaccination strategies with respect to the baseline strategy Pop. For this scenario, the effective reproduction number $R_{\text{eff}} = 1.0$ and the mobility factor $\tau = 0.5$.

Figure 23: Relative change in mortality for all vaccination strategies with respect to the baseline strategy `Pop`. For this scenario, the effective reproduction number $R_{\text{eff}} = 1.25$ and the mobility factor $\tau = 0.5$.

Figure 24: Relative change in new hospitalizations for all vaccination strategies with respect to the baseline strategy Pop. For this scenario, the effective reproduction number $R_{\text{eff}} = 1.25$ and the mobility factor $\tau = 0.5$.
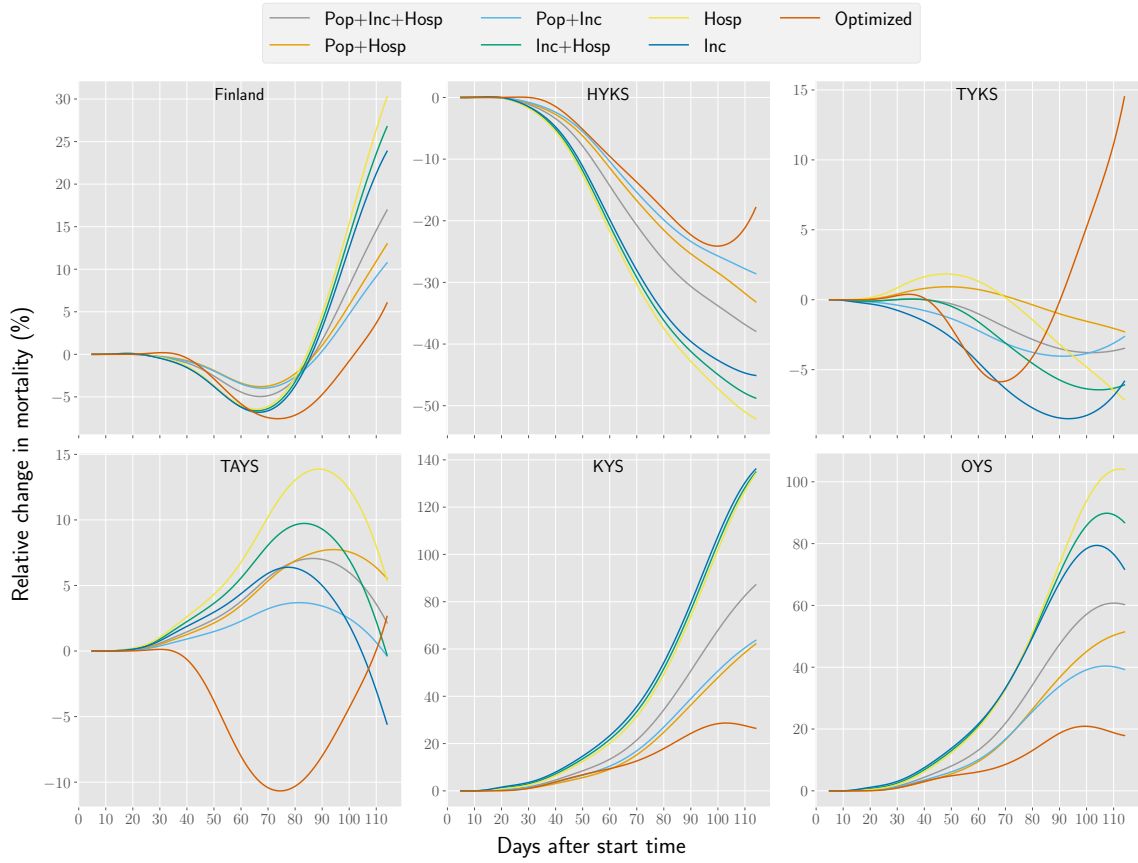
Figure 25: Relative change in incidence for all vaccination strategies with respect to the baseline strategy Pop. For this scenario, the effective reproduction number $R_{\text{eff}} = 1.25$ and the mobility factor $\tau = 0.5$.

Figure 26: Relative change in mortality for all vaccination strategies with respect to the baseline strategy Pop. For this scenario, the effective reproduction number $R_{\text{eff}} = 1.5$ and the mobility factor $\tau = 0.5$.
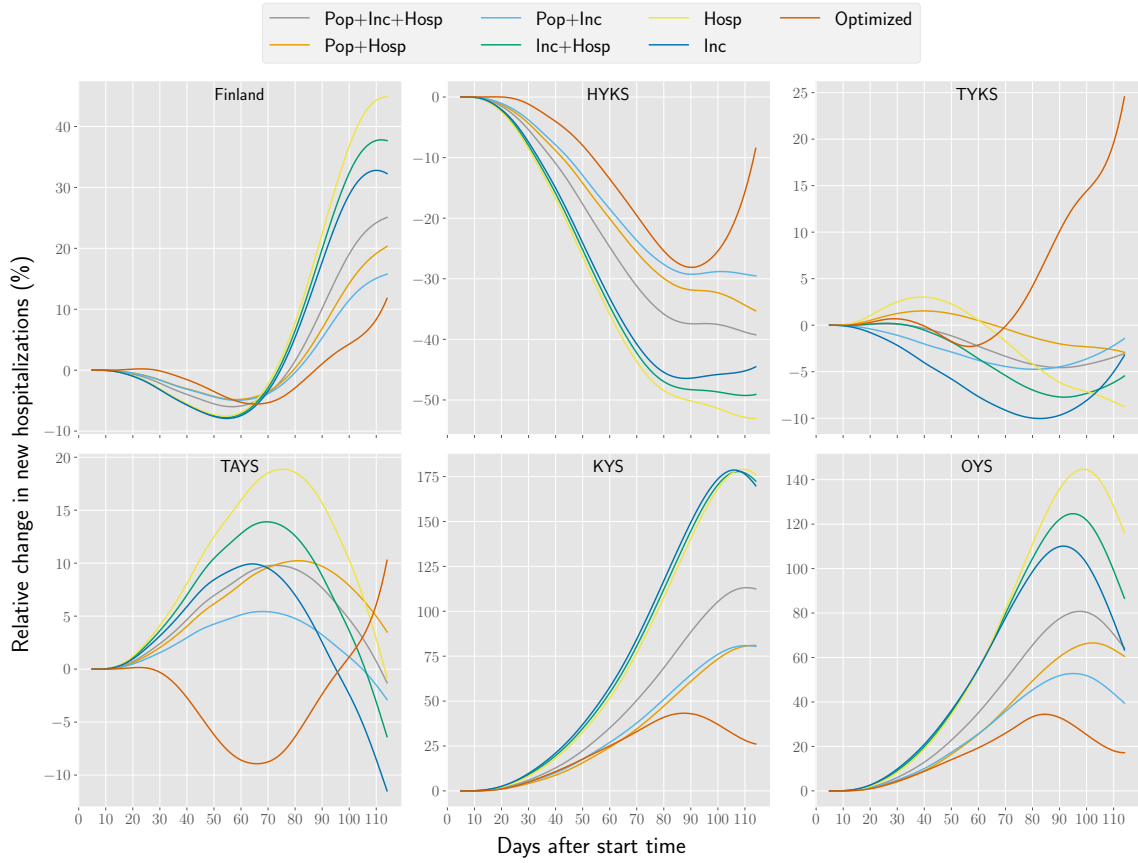
Figure 27: Relative change in new hospitalizations for all vaccination strategies with respect to the baseline strategy Pop. For this scenario, the effective reproduction number $R_{\text{eff}} = 1.5$ and the mobility factor $\tau = 0.5$.
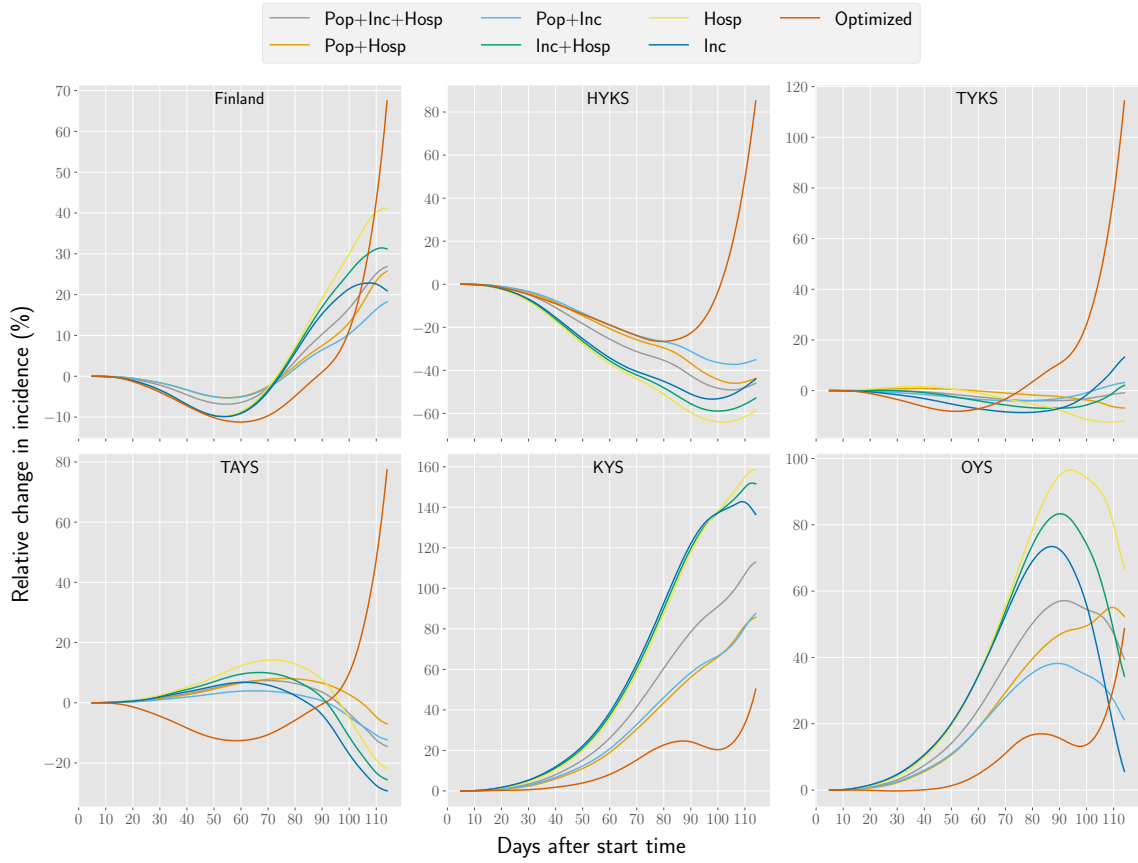
Figure 28: Relative change in incidence for all vaccination strategies with respect to the baseline strategy `Pop`. For this scenario, the effective reproduction number $R_{\mathrm{eff}} = 1.5$ and the mobility factor $\tau = 0.5$.